PHYSICS OF COMPACT OBJECTS
AND THEIR BINARY INTERACTIONS

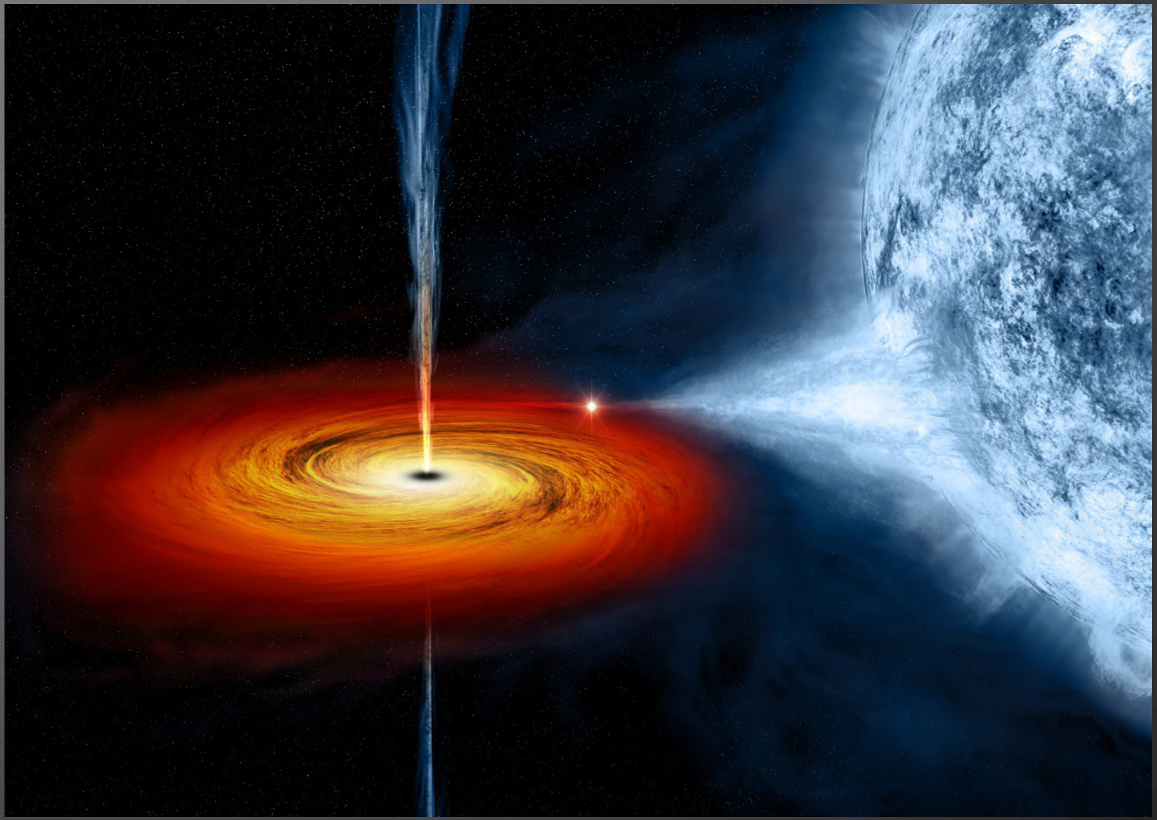

AALBORG UNIVERSITY

Thomas Tauris – Physics, Aalborg University

Programme

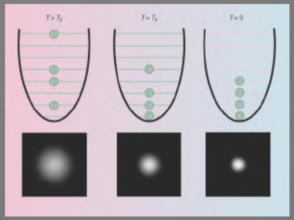


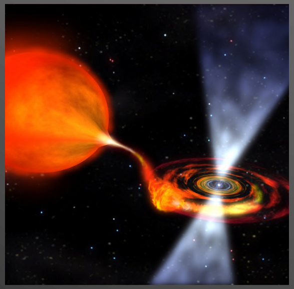
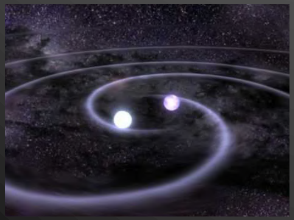

- ∗ **Introduction**
- ∗ **Degenerate Fermi Gases**

  Non-relativistic and extreme relativistic electron / (n,p,e^-) gases
- ∗ **White Dwarfs**

  Structure, cooling models, observations
- ∗ **Neutron Stars**

  Structure and equation-of-state
- ∗ **Radio Pulsars**

  Characteristics, spin evolution, magnetars, observations
- ∗ **Binary Evolution and Interactions**

  X-ray binaries, accretion, formation of millisecond pulsars, recycling
- ∗ **Black Holes**

  Observations, characteristics and spins
- ∗ **Gravitational Waves**

  Sources and detection, kilonovae
- ∗ **Exam**

Recyling MSPs
– accretion physics

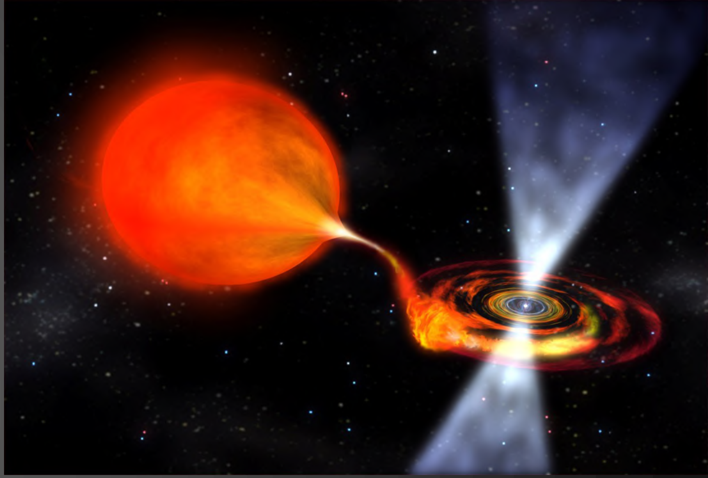

Last week

- Detailed LMXB evolution
  - dependence on P_{orb} and M_2
  - relation between M_{WD} and P_{orb} for binary pulsars
  - mass-transfer rate; final neutron star mass
  - equilibrium spin period and spin-up line in P-P_{dot} diagram

- Accretion physics
  - Four phases of accretion
  - (Accretion disks)
  - (Accretion-induced magnetic field decay)

Black Holes and their Spins

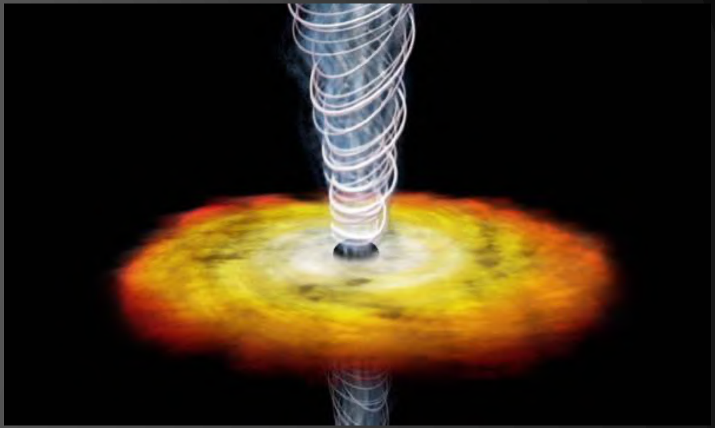

- Classification of BHs
  - Masses, radii, spins
  - BH anatomy
- Observations of BHs
  - Persistent sources
  - Transient sources
- BH spin measurements in X-ray binaries
  - Continuum fitting model
  - Innermost stable circular orbit (ISCO)
  - BH spin parameter
  - BH spectra
- BH spin and jets / mini-quasars
- BH mass determination

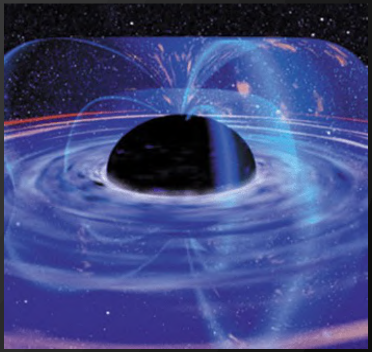

BH mergers detected by LIGO/Virgo/KAGRA are discussed next week.

Classification of Black Holes

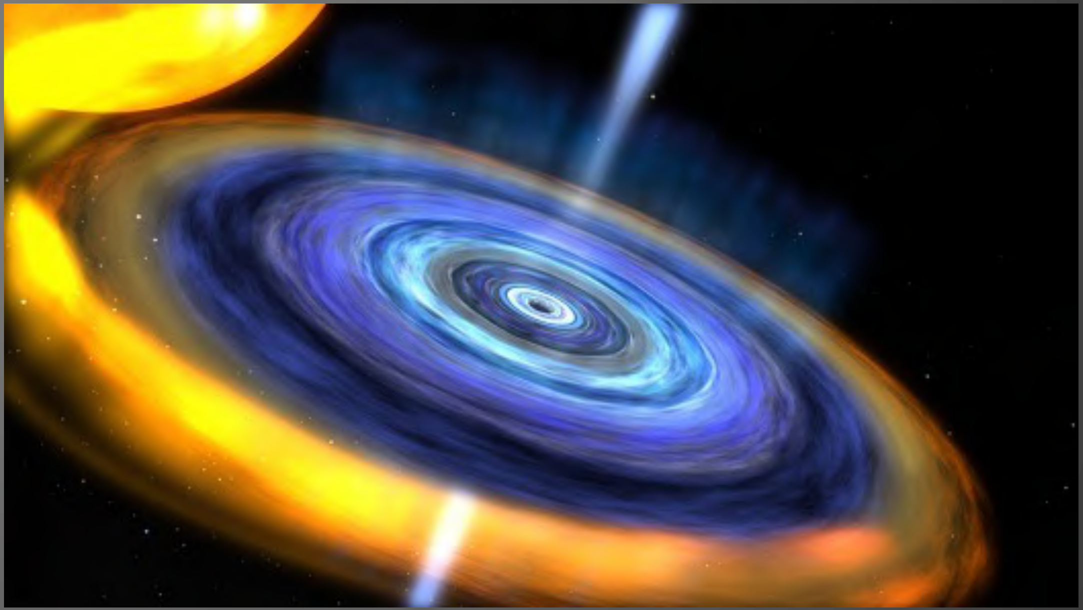

Black hole classifications			
Class	**Obs. evidence**	**Mass**	**Size**
Supermassive BH	YES	$\sim 10^5 – 10^{10}\ M_{sun}$	~ 0.001–400 AU
Intermediate mass BH	(yes?)	$\sim 10^3\ M_{sun}$	~ 1000 km
Stellar mass BH	YES	$\sim 10\ M_{sun}$	~ 30 km
Micro BH	NO	$\geq M_{Manhattan}$	≥ 2 mm

Classification of Black Holes

Only 3 externally observable parameters according to *no hair theorem:*

- mass
- spin (angular momentum)
- electric charge

It is likely that any natal BH **charge** will be neutralized by the surrounding medium

Four black hole solutions to the Einstein-Maxwell equations of gravitation and electromagnetism in general relativity:

Schwarzchild black hole:	no charge, no spin	(astrophysical)
Reissner-Nordström black hole:	charge, no spin	
Kerr black hole:	no charge, spin	(astrophysical)
Kerr-Newman black hole:	charge, spin	

Black Holes: masses, radii and spin

X-ray binaries in Milky Way:

Mass: "stellar mass black holes" have masses in the interval: $4 < M_{\rm BH}/M_\odot < 21$
determined via Kepler's 3. law in binaries

Radius: $$R_{sch} = \frac{2GM_{BH}}{c^2}$$

$$R_{sch} = 3\,km\ \ (M_{BH}/M_\odot)$$

Spin: $$0.1 < a_* < 0.99 \quad \wedge \quad a_* \equiv \frac{cJ}{GM^2}$$

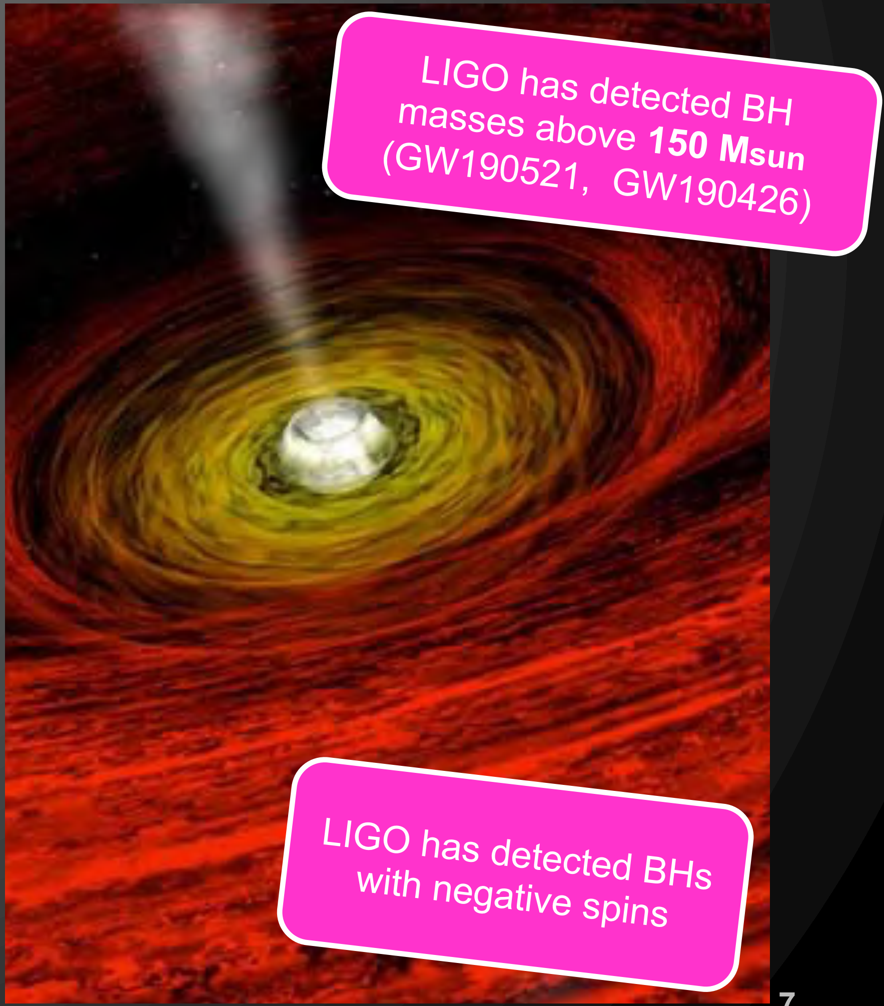

Evidence for existence: (BH vs NS)

- mass of compact object above NS threshold
- features of X-ray emission (hard surface or not)
- warping of spacetime in kHz QPOs
- gravitational waves detected by LIGO

The Schwarzchild radius defines the event horizon

Black Hole anatomy

Event horizon
A boundary beyond which events cannot affect an observer on the opposite side of it. Inside the event horizon no light can escape and all known physics breaks down.

Ergosphere
It is theoretically possible to extract energy and mass from this region.
Its outer boundary is defined as where a test particle moving at v=c would compensate frame-dragging and appear stationary for a distant observer.

Photon sphere
An area or region of space where gravity is so strong that photons are forced to travel in orbits.

ISCO (innermost stable circular orbit)
The smallest circular orbit in which a test particle can stably orbit a black hole.

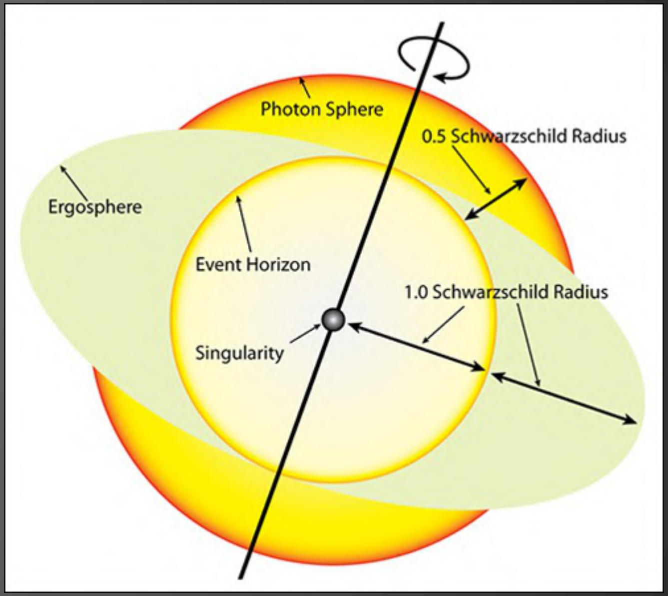

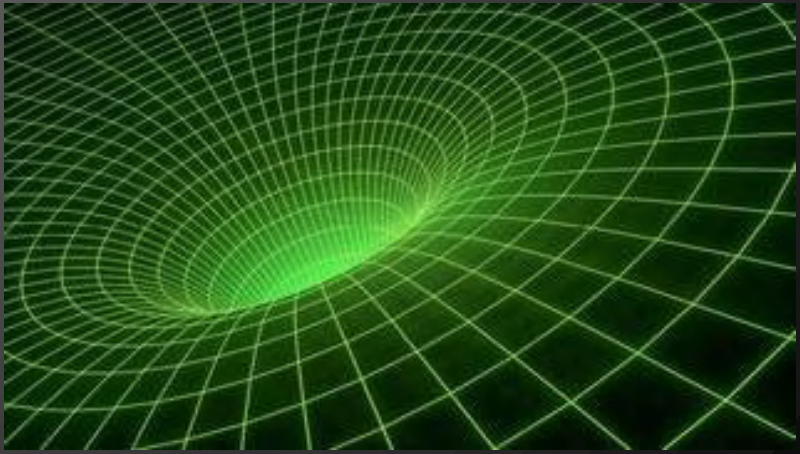

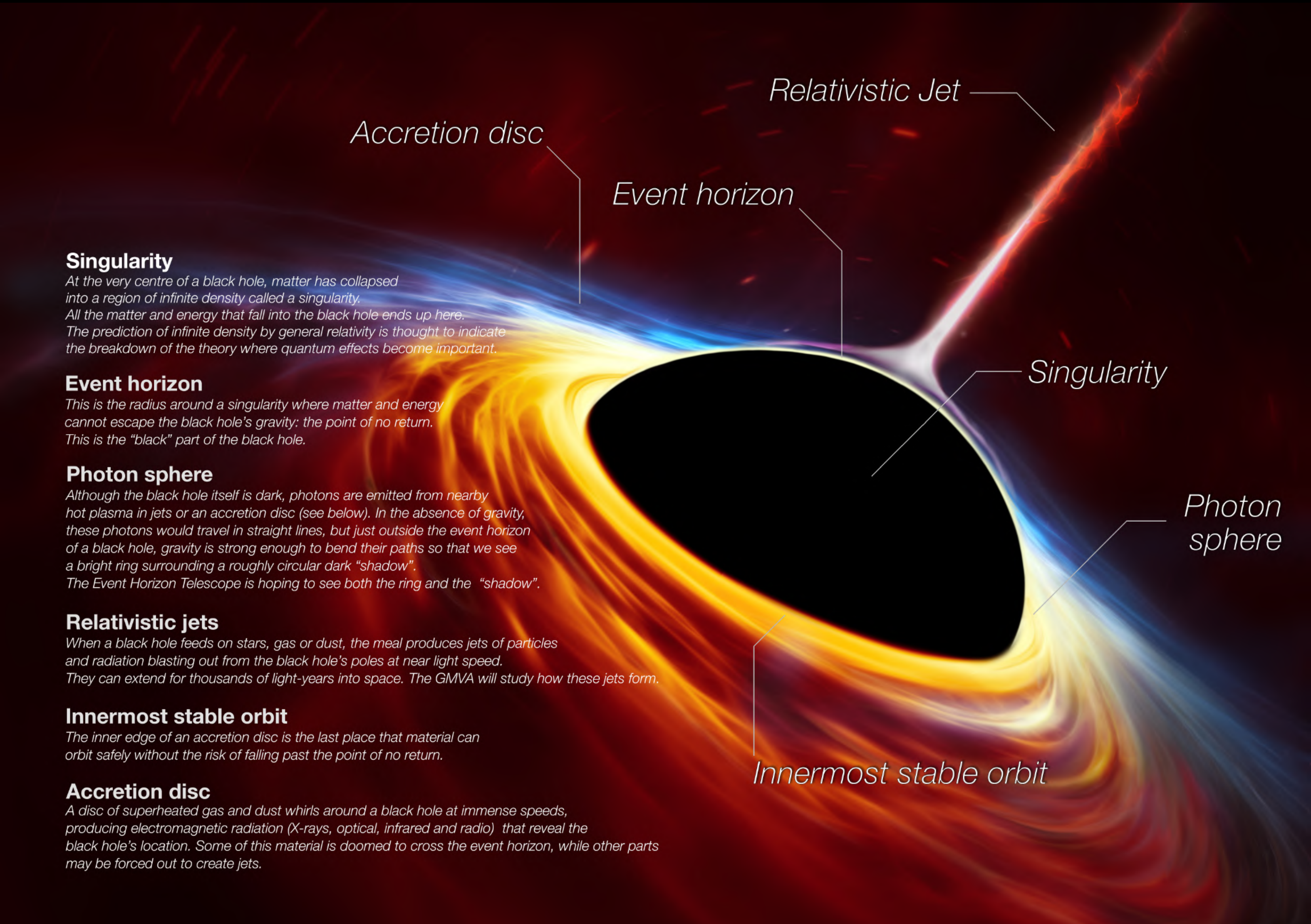

Singularity

At the very centre of a black hole, matter has collapsed into a region of infinite density called a singularity. All the matter and energy that fall into the black hole ends up here. The prediction of infinite density by general relativity is thought to indicate the breakdown of the theory where quantum effects become important.

Event horizon

This is the radius around a singularity where matter and energy cannot escape the black hole's gravity: the point of no return. This is the "black" part of the black hole.

Photon sphere

Although the black hole itself is dark, photons are emitted from nearby hot plasma in jets or an accretion disc (see below). In the absence of gravity, these photons would travel in straight lines, but just outside the event horizon of a black hole, gravity is strong enough to bend their paths so that we see a bright ring surrounding a roughly circular dark "shadow". The Event Horizon Telescope is hoping to see both the ring and the "shadow".

Relativistic jets

When a black hole feeds on stars, gas or dust, the meal produces jets of particles and radiation blasting out from the black hole's poles at near light speed. They can extend for thousands of light-years into space. The GMVA will study how these jets form.

Innermost stable orbit

The inner edge of an accretion disc is the last place that material can orbit safely without the risk of falling past the point of no return.

Accretion disc

A disc of superheated gas and dust whirls around a black hole at immense speeds, producing electromagnetic radiation (X-rays, optical, infrared and radio) that reveal the black hole's location. Some of this material is doomed to cross the event horizon, while other parts may be forced out to create jets.

Obs. of Accreting Black Holes

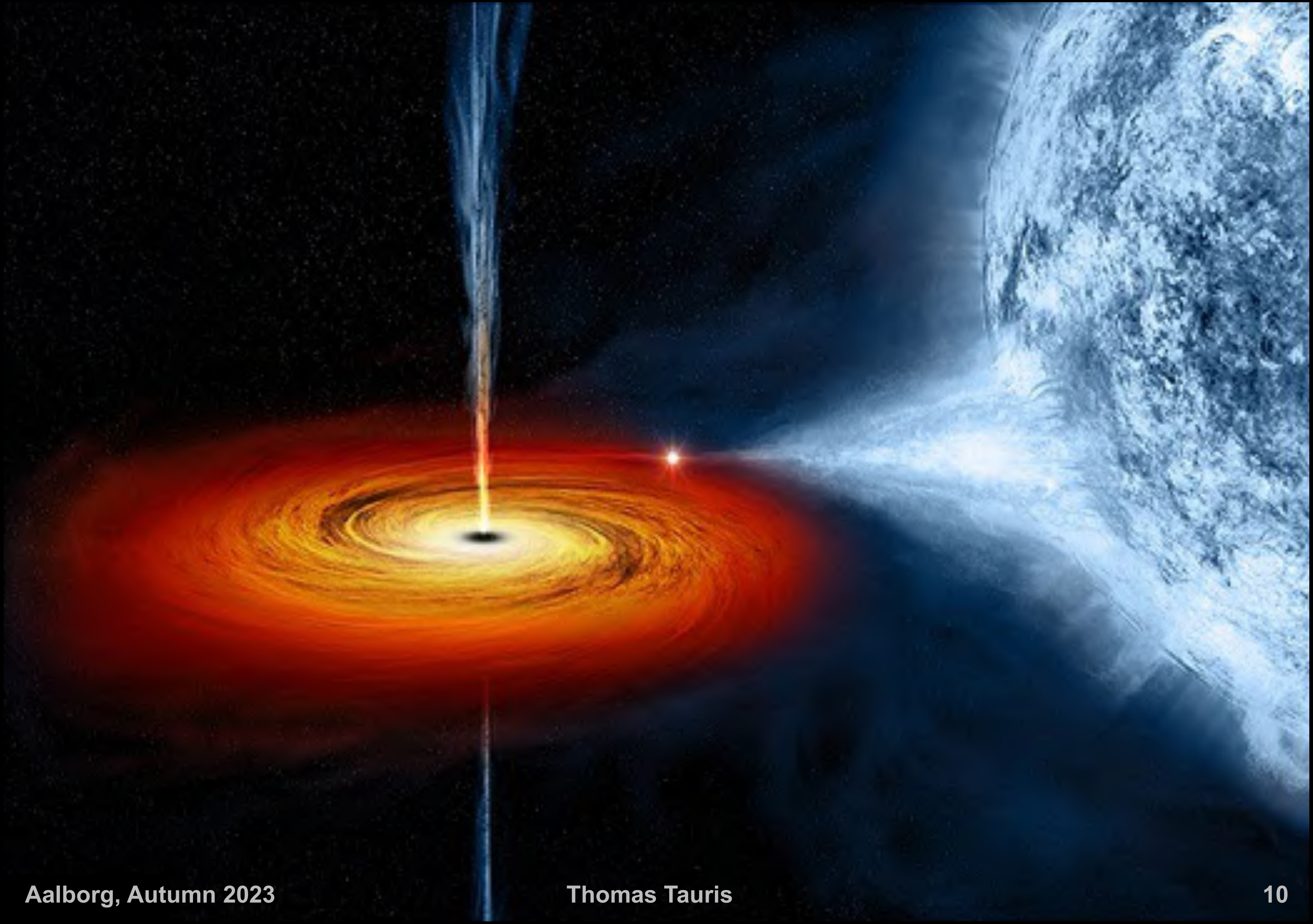

Observations of Stellar Mass Black Holes

Observations: Cygnus X-1, beginning of 1970's
Today: ~25 accreting stellar mass black holes are identified in the Milky Way and local galaxies

Uhuru

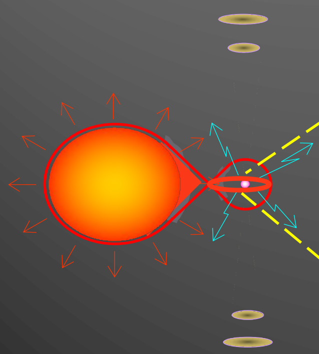

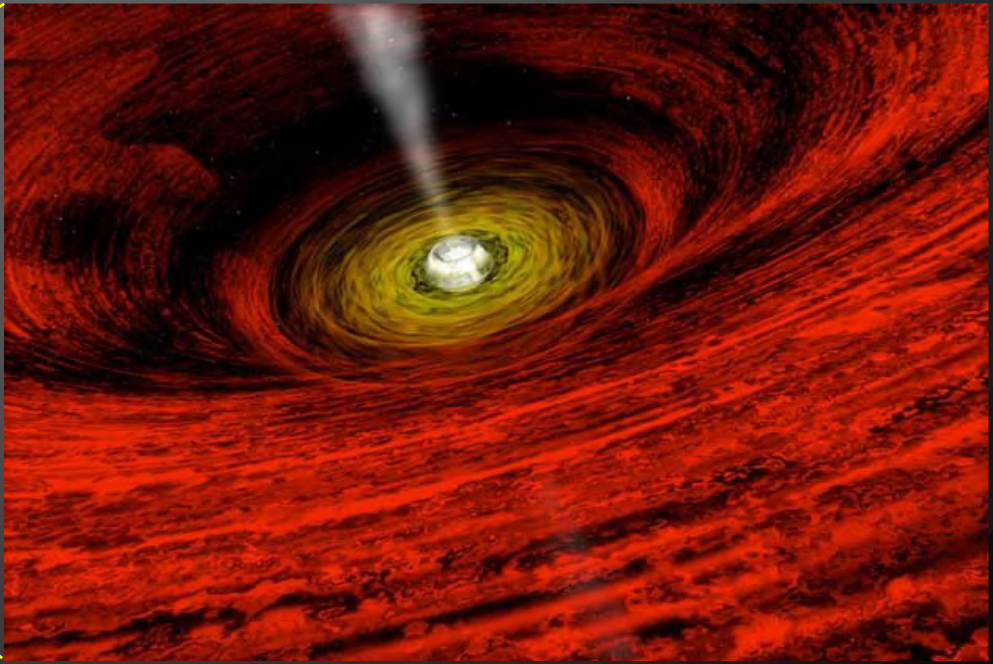

X-ray emission!!

Two classes of stellar mass BH binaries

4 systems with **wind-fed** accretion
Persistent sources

19 systems with **Roche-lobe overflow** accretion
Transient sources

Wind-fed / Persistent BH binaries

4 systems with **wind-fed** accretion

Persistent sources

Companion stars: $M_2 \approx 20-70\, M_\odot$ O-stars and Wolf-Rayet stars

Stellar wind mass loss: $\dot{M} \approx 10^{-5} - 10^{-8}\, M_\odot\, yr^{-1}$

Cyg X-1, LMC X-1, LMC X-3 and M33 X-7

Characterised by **large BH mass**: $M_{\mathrm{BH}} \approx 11 - 21\ M_\odot$

and **large spin**: $a_* \approx 0.84 - 0.99$

P_{orb} = 1.7–5.6 days

See e.g. Miller-Jones et al. (2021, Science) for Cyg X-1 mass and spin.

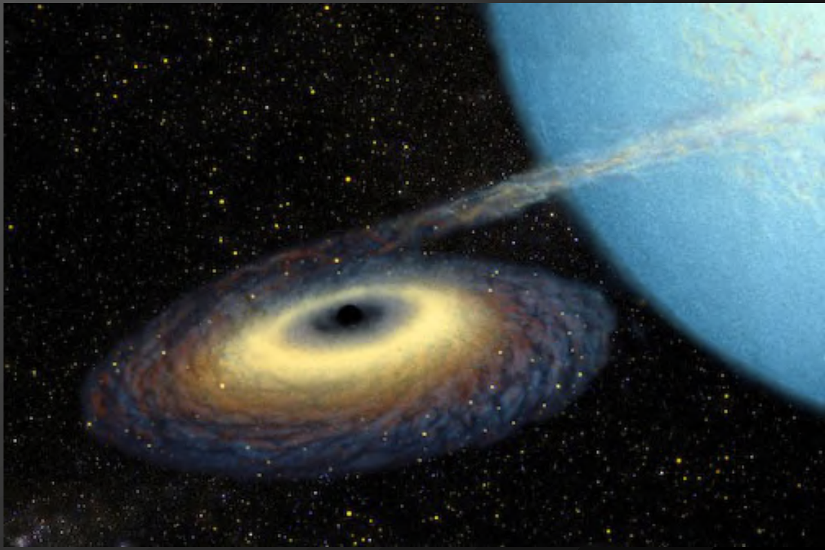

RLO / Transient BH binaries

19 systems with **Roche-lobe overflow** accretion

Transient sources

Companion stars: $M_2 \leq 1\,M_\odot$ (K-type dwarf / sub-giant) Soft-X-ray Transients (SXTs)

(Four oddballs with $M_2 = 2 - 6\,M_\odot$ including the mini-quasar GRS 1915+105)

X-ray luminosity: $L_{quiescent} \approx 10^{-6} L_{outburst} \quad \wedge \quad L_{outburst} \approx L_{Edd} \approx 10^{39}\ erg\ s^{-1}$

Characterised by **small BH mass**: $M_{BH} \approx 4 - 10\,M_\odot$

and **small/medium/large spin**: $a_* = 0.10 - 0.95$

P_{orb} = 0.17–33 days

One Be/X-ray binary with a BH

Until 2014, all ~80 known Be/X-ray binaries had a NS companion!

Beware:
Janssens et al. (2023) presented evidence that MWC 656 is a Be+NS

MWC 656 (Casares et al. (2014), Nature 505, 378)

Orbital period: $P_{orb} = 60\ days$

Companion star: $M_2 = 10 - 16\ M_{\odot}$ (Be-star)

Radial velocity measurements: $q = M_{BH} / M_2 = 0.41 \pm 0.07$

Mass of BH: $M_{BH} \approx 3.8 - 6.9\ M_{\odot}$

X-ray luminosity: inefficient accretion in quiescent state: $L_{quiescent} \approx 10^{-7}\ L_{Edd}$

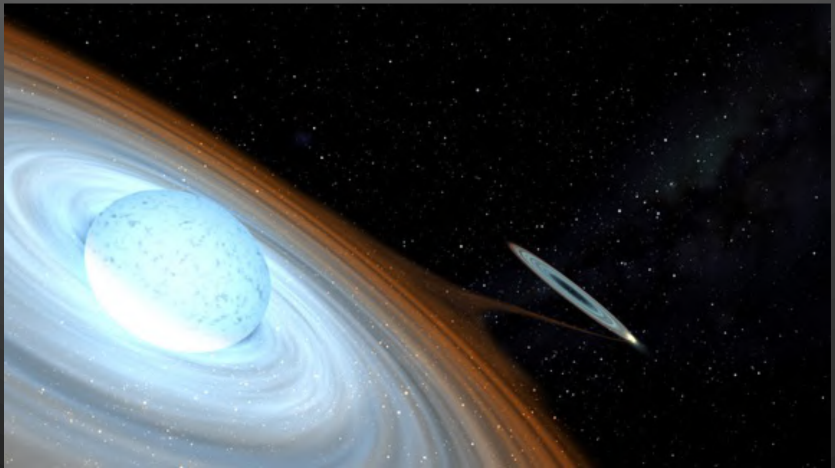

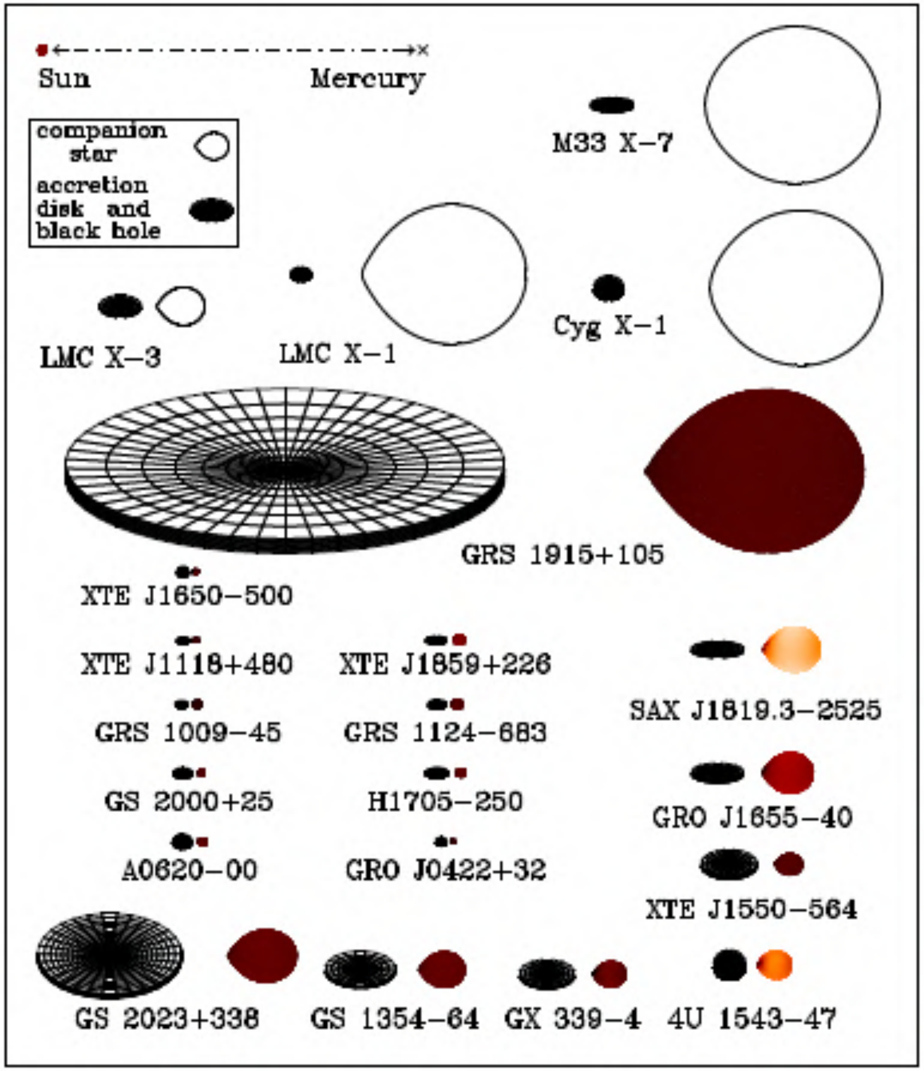

Fig. 1 Schematic sketch to scale of 21 black hole binaries (see scale and legend in the upper-left corner). The tidally-distorted shapes of the companion stars are accurately rendered in Roche geometry. The black holes are located in the center of the disks. A disk's tilt indicates the inclination angle i of the binary, where $i = 0$ corresponds to a system that is viewed face-on; e.g., $i = 21°$ for 4U 1543–47 (bottom right) and $i = 75°$ for M33 X-7 (top right). The size of a system is largely set by the orbital period, which ranges from 33.9 days for the giant system GRS 1915+105 to 0.2 days for tiny XTE J1118+480. Three well-studied persistent systems with their supergiant secondaries are located in the upper-right corner. (Figure courtesy of J. Orosz.)

An astrophysical BH is completely described by M and J

(given that Q=0 via surrouding medium)

$$a_* \equiv \frac{a}{M} = \frac{J\,c}{GM^2}$$ the dimensionless spin parameter

$$a_* = 0 \quad (\text{Schwarzchild BH})$$
$$a_* = 1 \quad (\text{maximally rotating BH})$$

The BH spin parameter provides information about:

– BH formation process

(angular momentum of progenitor stars, GRBs)

– BH spin evolution

(connection to accretion (spin-up?) and relativistic jets (spin-down?))

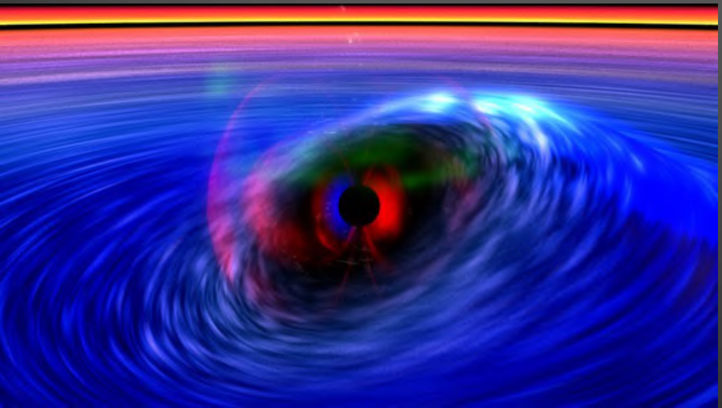

$$E_{spin} \sim 0.30\, Mc^2 \quad (a_* = 1)$$

Space around a spinning BH

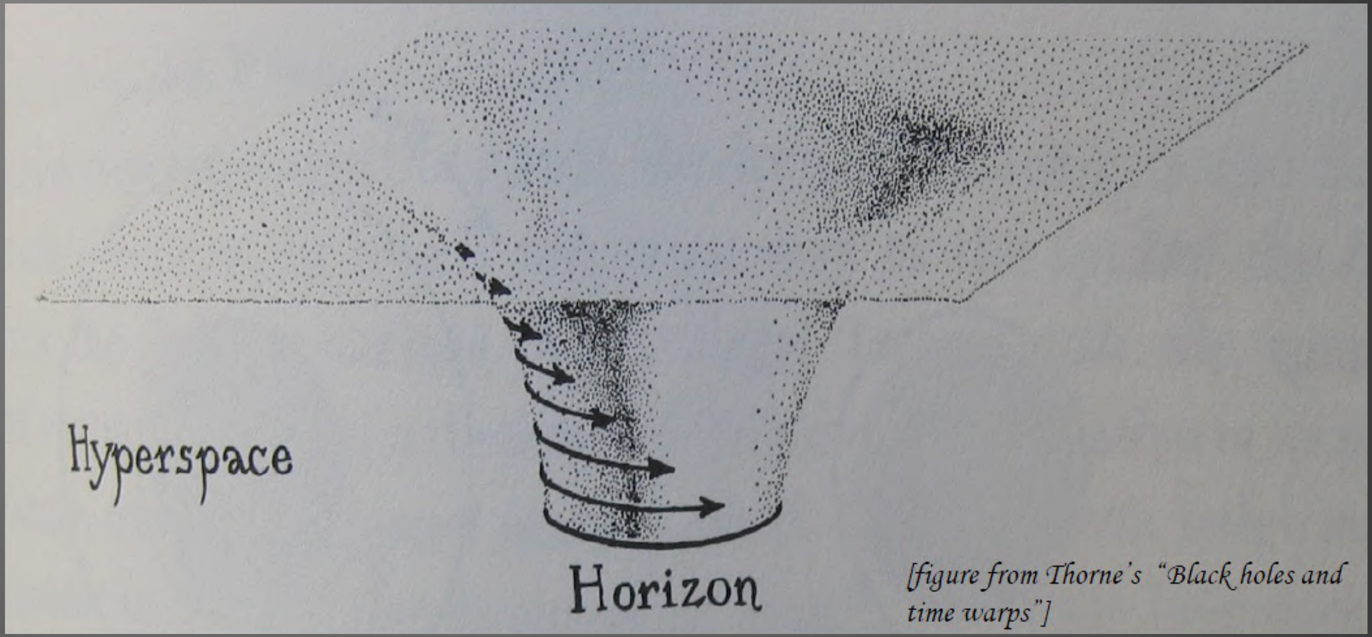

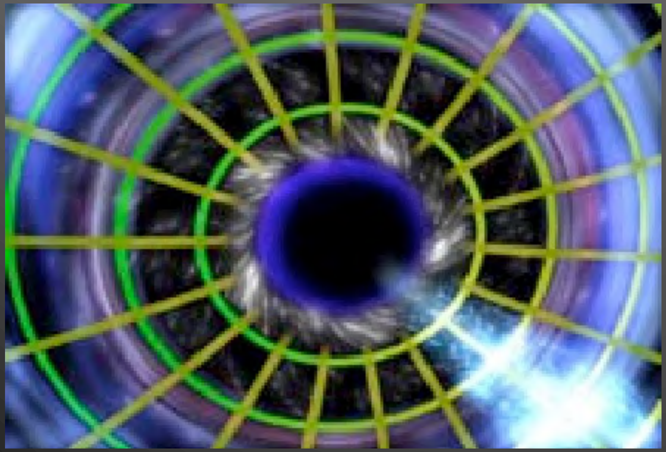

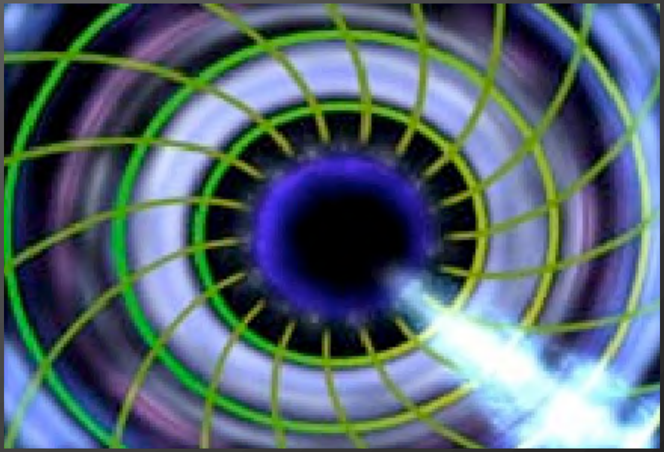

© NASA

Non-spinning BH

Spinning BH (frame dragging)

Frame dragging and particle trajectories:

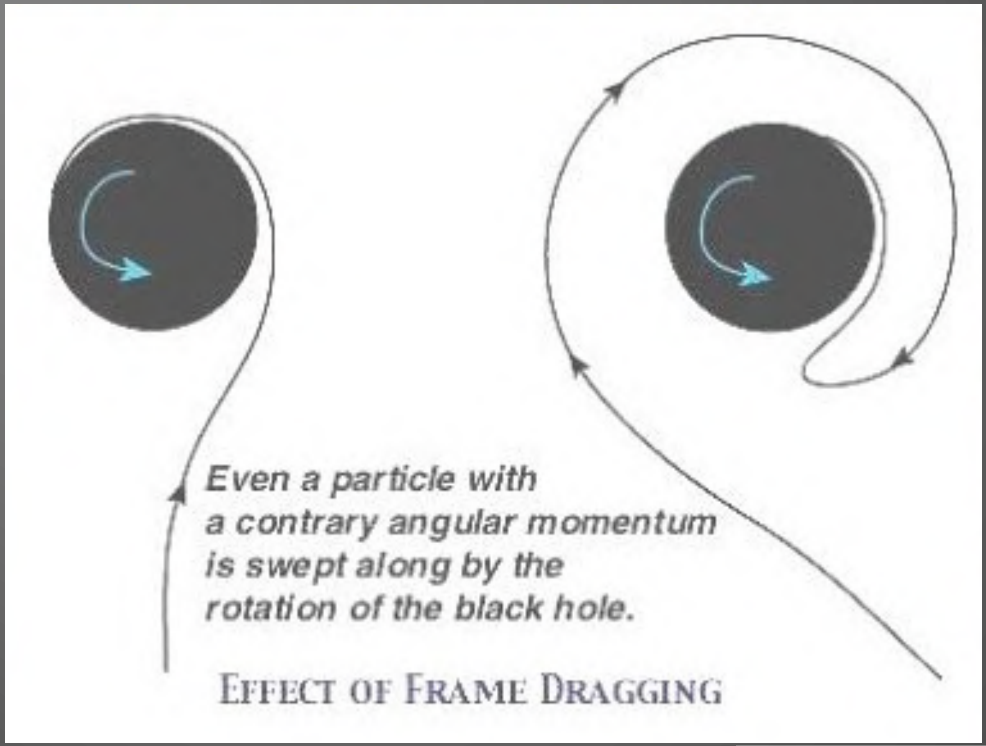

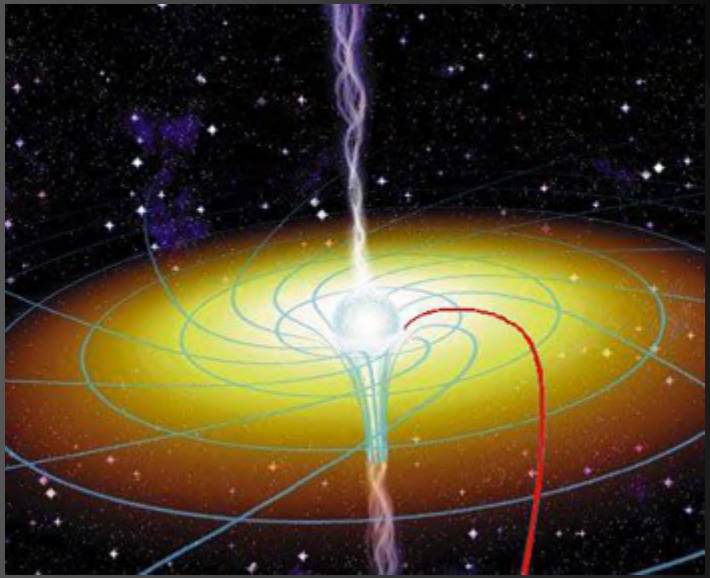

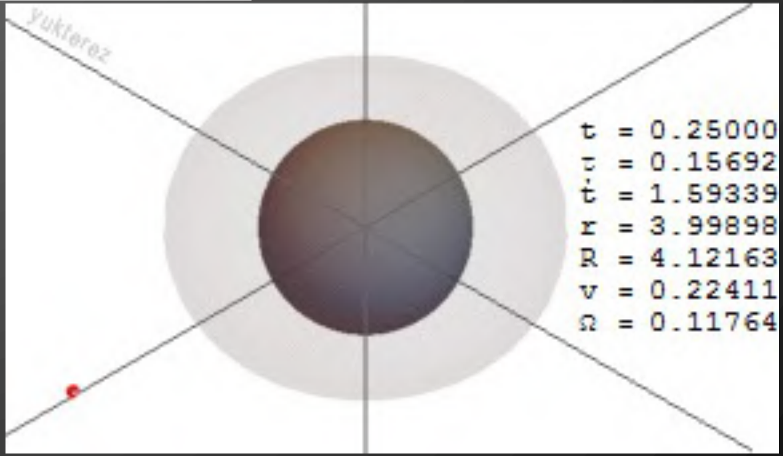

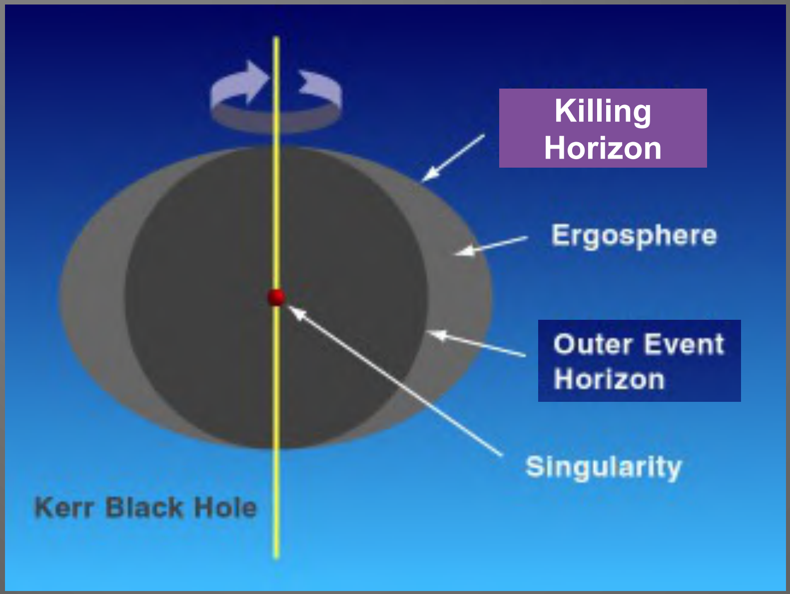

No signal can escape the event horizon.

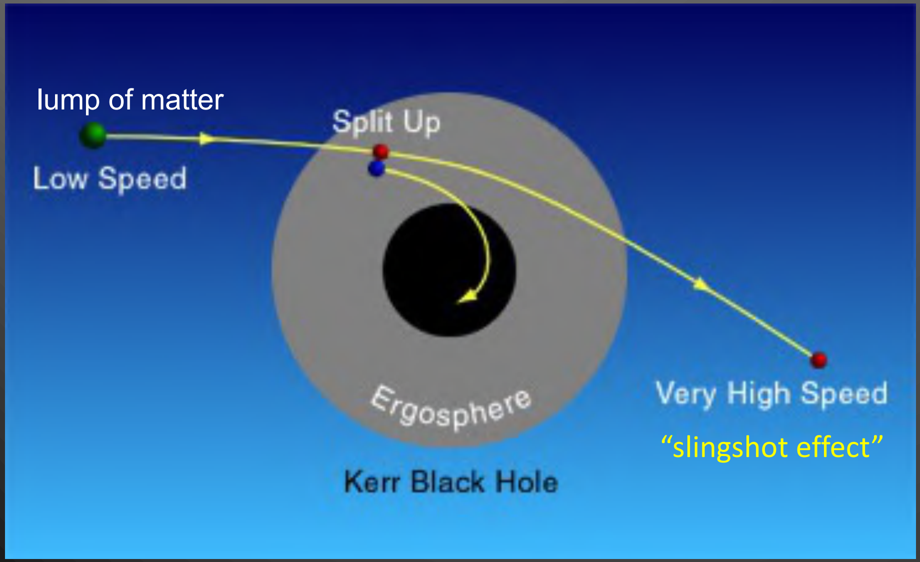

Inside the ergosphere spacetime is dragged along, causing matter being forced to corotate. In principle, rotational energy of the BH can be extracted from the ergosphere by the Penrose (1969) process.

The Penrose process can extract rotational energy from a BH (see Shapiro & Teukolsky p.363).

The BH spin can be estimated in X-ray binaries via:

1. X-ray continuum spectrum (e.g. McClintock, Narayan & Steiner 2013)
2. Relativistically broadened iron line (e.g. Reynolds 2013)
3. Quasi-periodic oscillations (e.g. Dokuchaev 2013, Motta et al. 2014, 2022)

By measuring the radius of the innermost stable circular orbit, R_{ISCO} one can obtain the spin parameter a_*

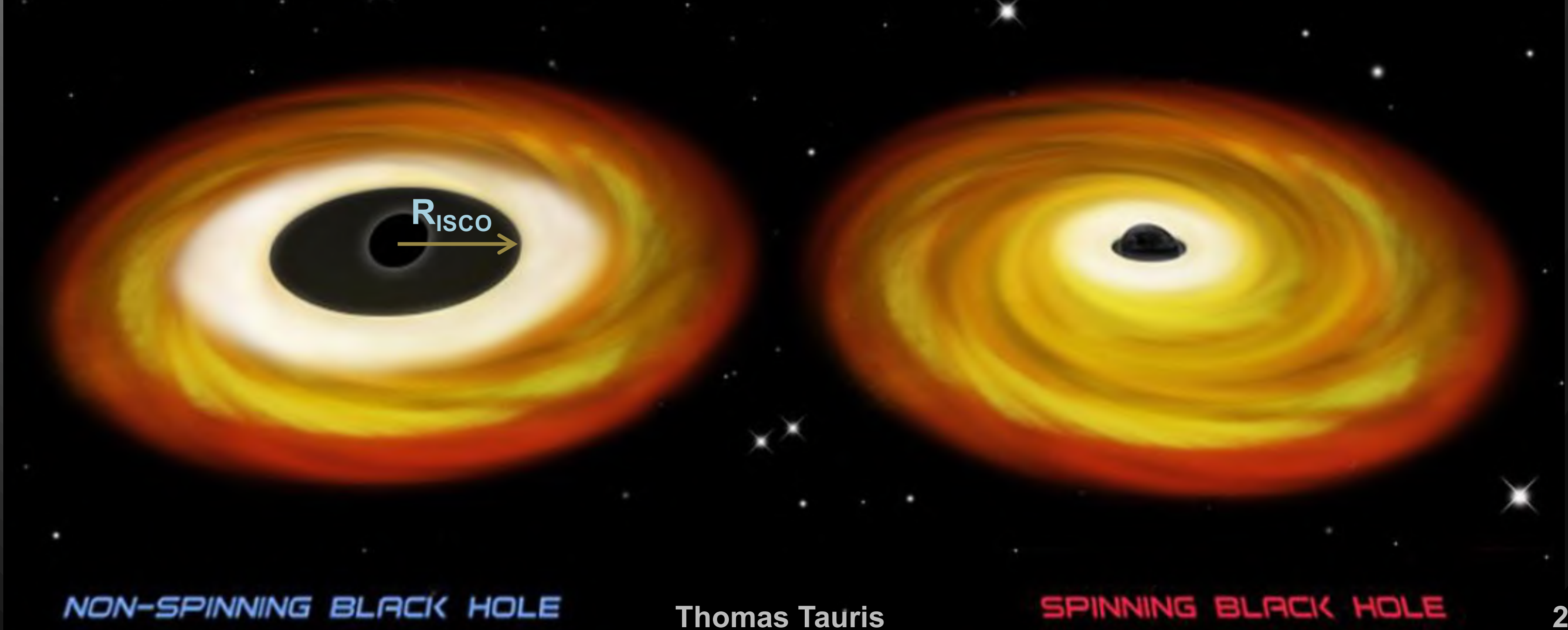

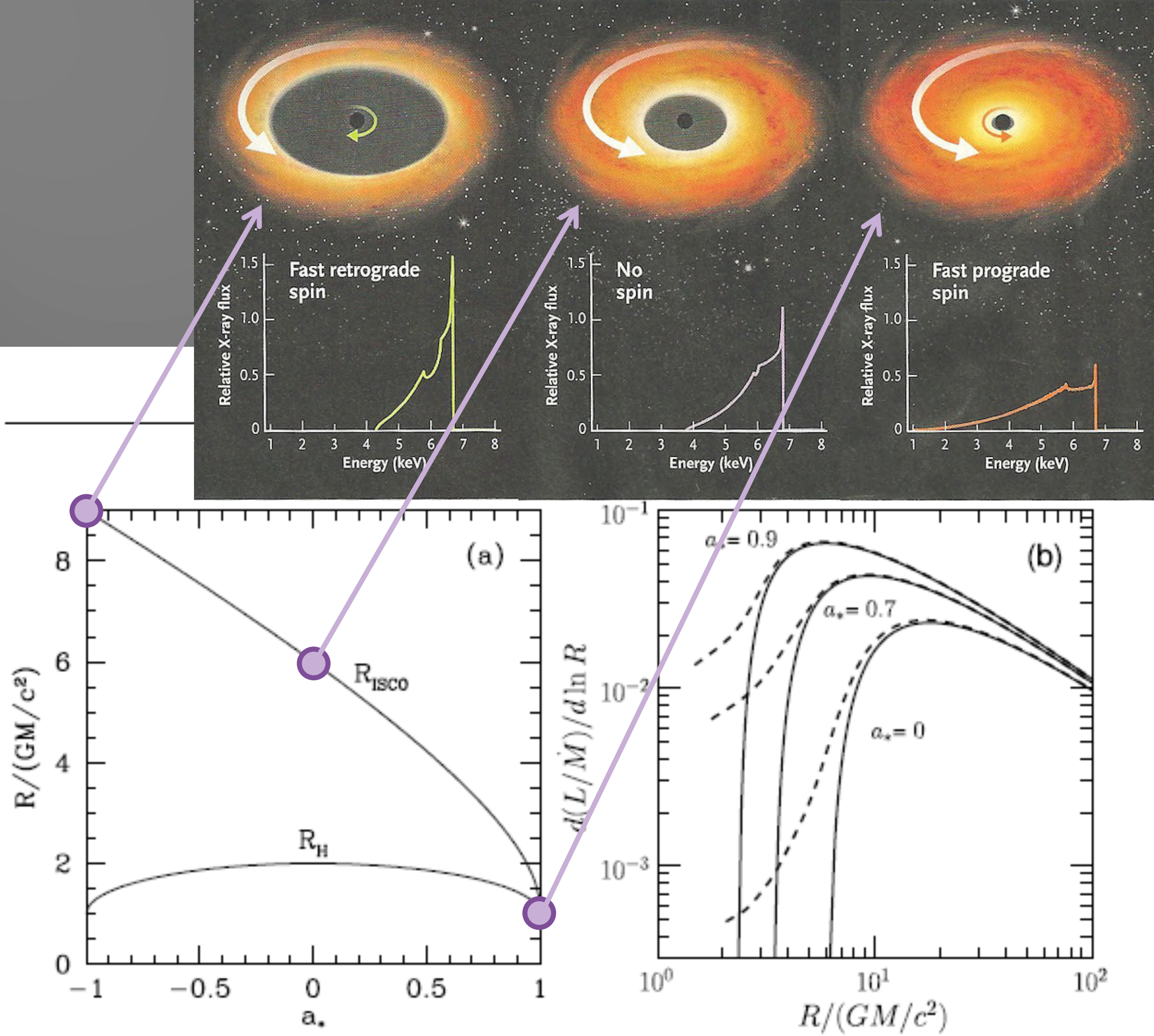

$$R_{isco} = \begin{cases} 9\ GM/c^2 & a_* = -1 \\ 6\ GM/c^2 & a_* = 0 \\ 1\ GM/c^2 & a_* = 1 \end{cases}$$

$$R_H = \begin{cases} 1\ GM/c^2 & a_* = -1 \\ 2\ GM/c^2 & a_* = 0 \\ 1\ GM/c^2 & a_* = 1 \end{cases}$$

Fig. 3 (a) Radius of the ISCO $R_{\rm ISCO}$ and of the horizon $R_{\rm H}$ in units of GM/c^2 plotted as a function of the black hole spin parameter a_*. Negative values of a_* correspond to retrograde orbits. Note that $R_{\rm ISCO}$ decreases monotonically from $9GM/c^2$ for a retrograde orbit around a maximally spinning black hole, to $6GM/c^2$ for a non-spinning black hole, to GM/c^2 for a prograde orbit around a maximally spinning black hole. (b) Profiles of $d(L/\dot{M})/d\ln R$, the differential disk luminosity per logarithmic radius interval normalized by the mass accretion rate, versus radius $R/(GM/c^2)$ for three values of a_*. Solid lines are the predictions of the NT model. The dashed curves from Zhu et al. (2012), which show minor departures from the NT model, are discussed in Section 5.2.

The disk spectrum
(peak emission and temperature)
depends on $R_{\rm ISCO}$.

Hence, $R_{\rm ISCO}$ and thus a_* can be determined from continuum fitting.

The solution to Einstein's equations for a rotating BH was discovered by Kerr (1963). Here shown in Boyer-Lindquist (1967) coordinates, in which the line element is given by (Shapiro & Teukolsky, Chap.12):

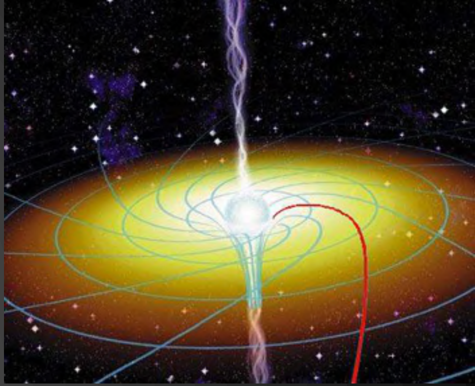

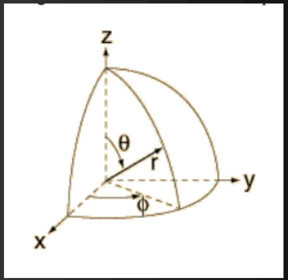

$$ds^2 = -\left(1 - \frac{2Mr}{\Sigma}\right)dt^2 - \frac{4aMr\sin^2\theta}{\Sigma}\,dt\,d\phi + \frac{\Sigma}{\Delta}dr^2 + \Sigma\,d\theta^2 + \left(r^2 + a^2 + \frac{2Mra^2\sin^2\theta}{\Sigma}\right)\sin^2\theta\,d\phi^2 \qquad (12.7.1)$$

where the BH is spinning in the ϕ direction, and

$$a \equiv \frac{J}{M}, \qquad \Delta \equiv r^2 - 2Mr + a^2, \qquad \Sigma \equiv r^2 + a^2\cos^2\theta, \qquad (\text{note} \quad G = c = 1)$$

$$\wedge \quad a_* \equiv \frac{a}{M} \quad \left(a_* = \frac{J\,c}{GM^2}\right) \quad !$$

Setting a=0 yields the Schwarzchild metric for a non-spinning BH. The $dt\,d\phi$ term shows the rotational frame-dragging properties of a spinning BH.

The event horizon, R_H is found when the dr^2 term in the line element becomes singular, i.e. when $\Delta=0$, or:

$$R_{H\pm} = M \pm \sqrt{M^2 - a^2}$$

kan nemt verificeres

$$a_* = 0 \quad \Rightarrow \quad \{R_{H+} = 2M, \quad R_{H-} = 0\}$$
$$a_* = 1 \quad \Rightarrow \quad \{R_{H+} = R_{H-} = M\}$$

Note, only R_{H+} has an astrophysical meaning.

The effective potential felt by particles orbiting a BH is given by:

$$V \equiv E^2\left(r^3 + a^2 r + 2Ma^2\right) - 4aMEl - (r-2M)l^2 - m^2 r\Delta \qquad (12.7.15)$$

where E, l and m are the binding energy, ang. mom. and particle mass.

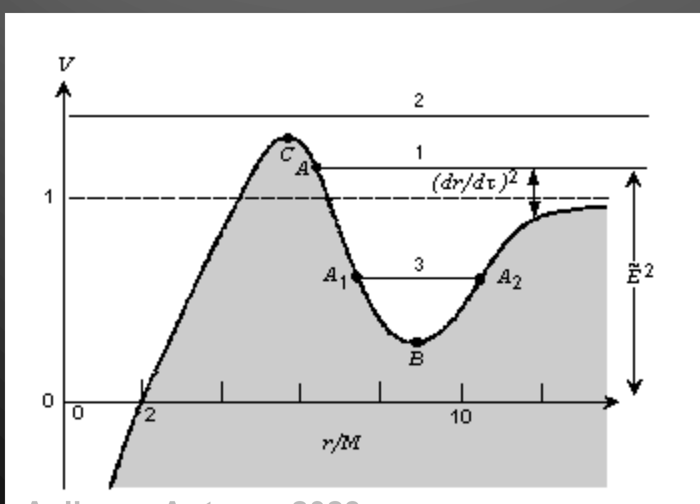

non-radial motion of test particles (S&T Fig.12.2)

2. goes straight into BH (capture)

1. bounces off and escapes BH (unbound)

3. trapped orbit around BH (bound)

B. Stable circular orbit
C. Unstable circular orbit

For circular orbits, the specific energy and the specific ang. mom. are:

$$\frac{E}{m} = \frac{r^2 - 2Mr \pm a\sqrt{Mr}}{r\sqrt{r^2 - 3Mr \pm 2a\sqrt{Mr}}} \qquad (12.7.17)$$

$$\frac{l}{m} = \frac{\sqrt{Mr}\left(r^2 \mp 2a\sqrt{Mr} + a^2\right)}{r\sqrt{r^2 - 3Mr \pm 2a}} \qquad (12.7.18)$$

The so-called photon radius is a singularity in the above equations (solving for the denominators being equal to zero):

$$r_{ph} = 2M\left\{1 + \cos\left[\frac{2}{3}\cos^{-1}\left(\mp a / M\right)\right]\right\} \qquad (12.7.21)$$

$$a_* = \{-1, 0, 1\} \quad \Rightarrow \quad r_{ph} = \{4M, 3M, 1M\}$$

A **photon sphere** is a spherical region of space where gravity is strong enough that photons are forced to travel in orbits.

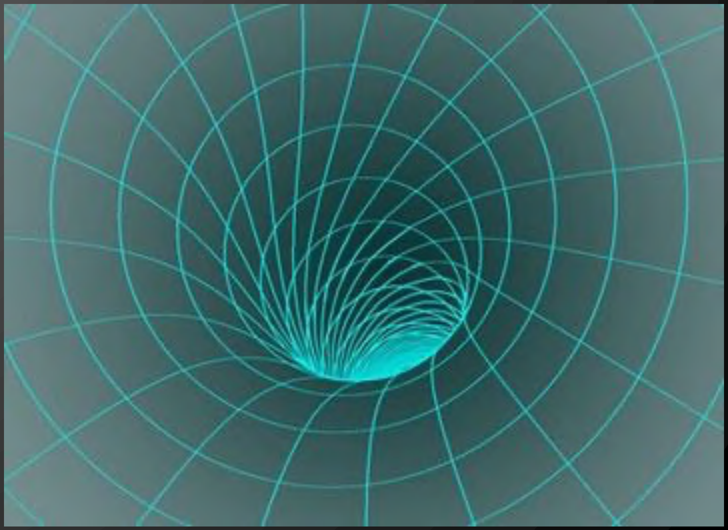

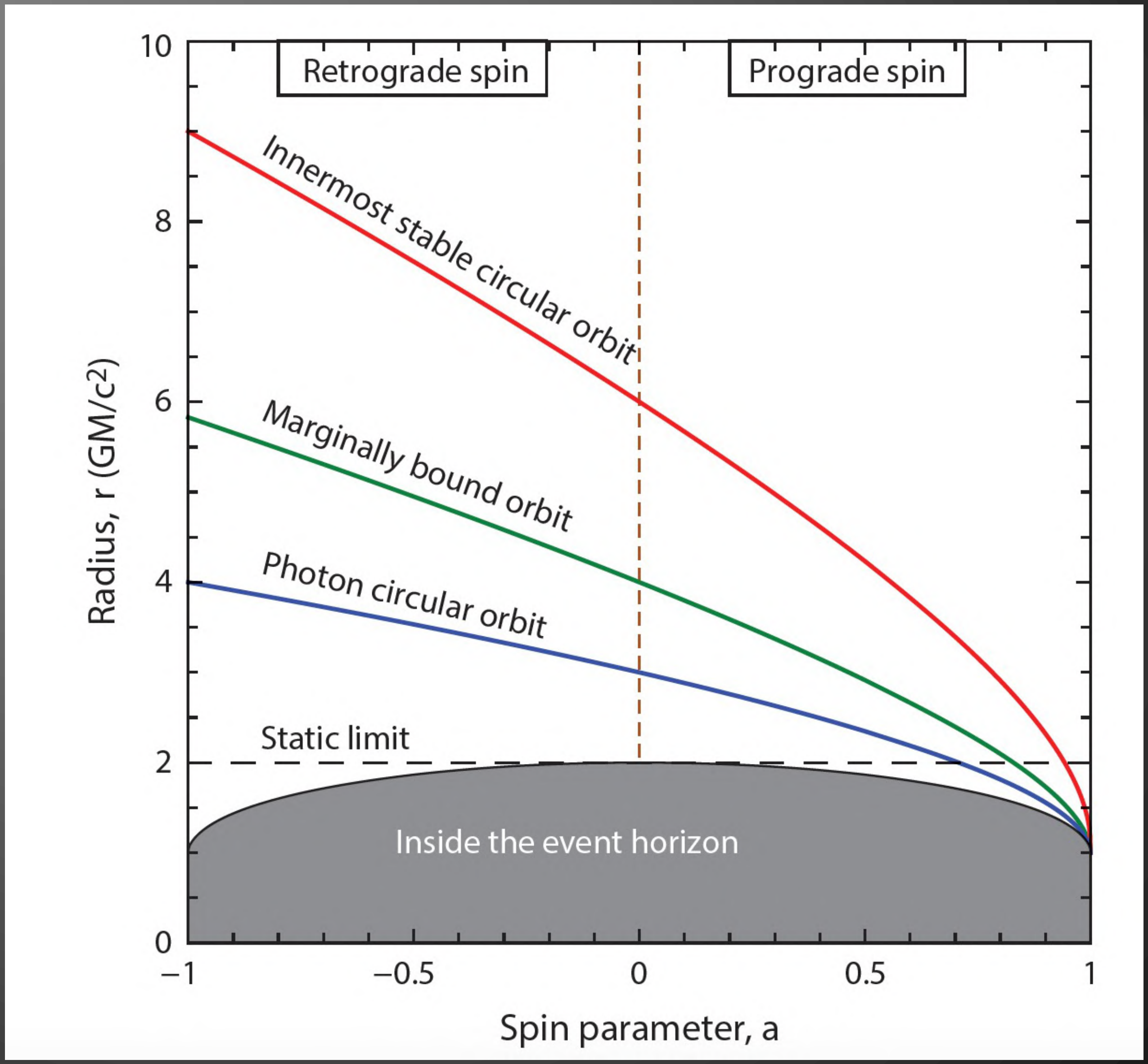

Reynolds (2021)

In GR, circular orbits can exist from $r = \infty$ to $r = r_{ph}$, and these can be both bound or unbound. Furthermore, not all bound orbits are *stable*. Using the stability criterion: $\partial^2 V/\partial r^2 = 0$ yields (after some algebra!):

$$R_{isco} = M\left\{3 + Z_2 \mp \left[(3 - Z_1)(3 + Z_1 + 2Z_2)\right]^{1/2}\right\} \quad (12.7.24)$$

$$Z_1 \equiv 1 + \left(1 - a^2/M^2\right)^{1/3}\left[\left(1 + a/M\right)^{1/3} + \left(1 - a/M\right)^{1/3}\right],$$

$$Z_2 \equiv \left(3a^2/M^2 + Z_1^2\right)^{1/2}$$

Innermost Stable Circular Orbit (ISCO)

Bardeen (1972)

$$a_* = \{-1, 0, 1\} \quad \Rightarrow \quad R_{isco} = \{9M, 6M, 1M\}$$

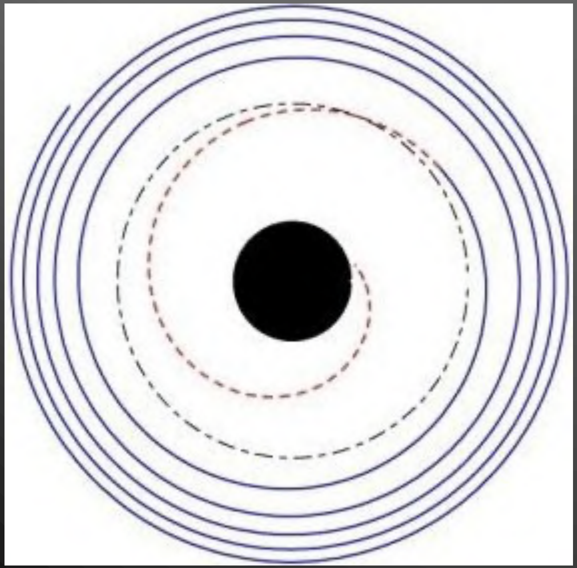

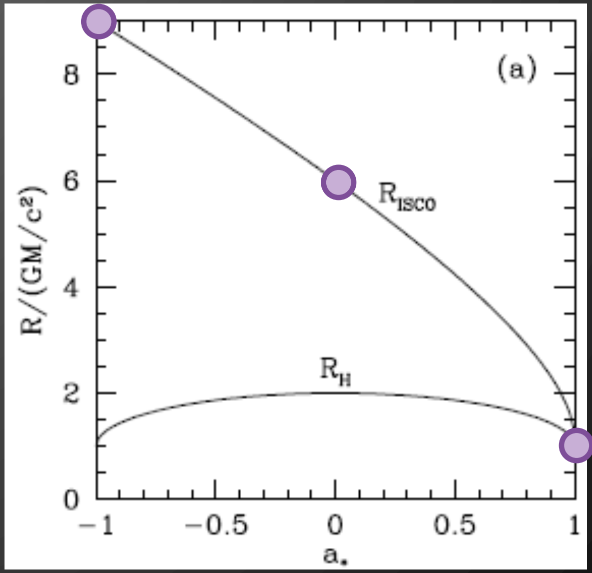

The binding energy* at the ISCO is important for the accretion luminosity:

$$a_* = \frac{a}{m} = \mp \frac{4\sqrt{2}\sqrt{1-(E/m)^2} - 2E/m}{3\sqrt{3}\left(1-(E/m)^2\right)} \qquad (12.7.25)$$

plus

$$a_* = \{-1, 0, 1\} \quad \Rightarrow \quad E/m = \left\{\sqrt{25/27}, \sqrt{8/9}, \sqrt{1/3}\right\}$$

Realistic accretion disks with B-fields may change this slightly…

Thus the maximum energy release is: $1-\sqrt{1/3} \approx 0.423$ of rest-mass energy!

(For a non-spinning BH the energy release is: $1-\sqrt{8/9} \approx 0.057$)

* Defined to be zero at event horizon? (and not at infinity? Hence, $1-E/m$?)

Black hole spectrum

Depends on accretion disk geometry

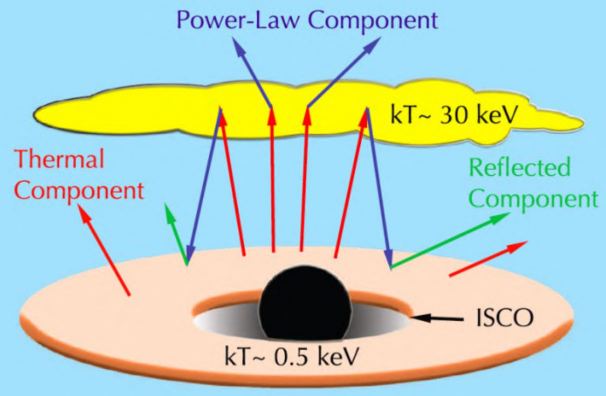

Black body-like thermal component.

Compton scattering of photons off the hot electrons (Poutanen et al. 2018).

Reflection of the corona radiation by the underlying disk (Fabian et al. 2000).

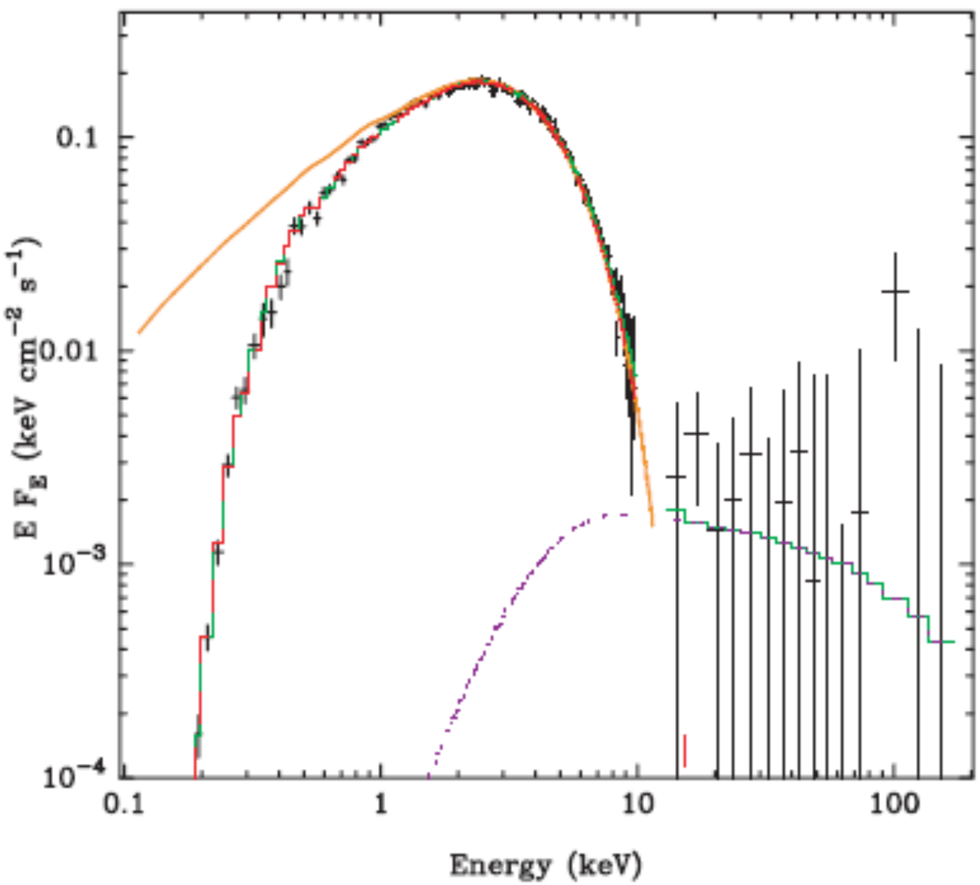

Fig. 4 Model fit to a disk-dominated spectrum of LMC X-3 obtained using detectors aboard the *BeppoSAX* satellite for $D = 52$ kpc, $i = 67°$ and $M = 10\,M_\odot$ (Davis et al. 2006). A green solid curve, which is difficult to discern because it hugs the data, is the total model. Also shown is the thermal component (red long-dashed curve) and the Compton component (violet short-dashed curve). The reflected component is negligible and was not included. The orange solid curve shows the total model with the effects of interstellar absorption removed. Note that the peak Compton flux is only 1% of the peak thermal flux.

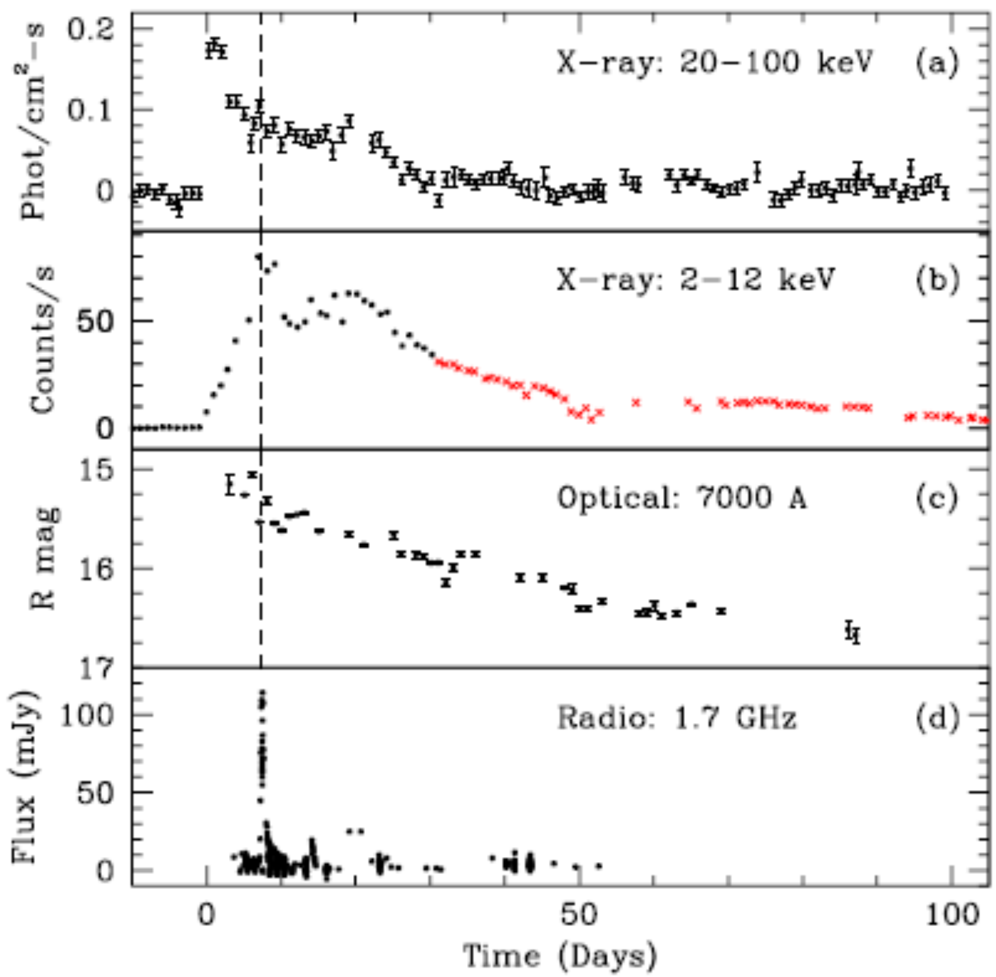

Fig. 2 Outburst cycle of XTE J1859+226 in 1999. The dashed line (top three panels) marks the time of peak radio flux (panel d). The ≈ 1-day radio spike (panel d) is shown fully resolved in Figure 2 in Brocksopp et al. (2002). The red crosses (panel b) indicate times when the X-ray spectrum is dominated by the thermal component. These *BATSE* and *RXTE*/ASM X-ray, and Merlin (and other) radio data (panels a, b and d, respectively) appear in Figure 1 in Brocksopp et al. (2002) and the optical data (panel c) appear in Figure 2 in Sánchez-Fernández et al. (2001). For further details, consult the references.

Successful application of the continuum-fitting method requires spectra with a substantial thermal component and $L/L_{Edd} < 0.3$. Otherwise, the thin disk model is invalidated.

The constancy of R_{in} suggests that this fitted parameter is indeed related to the R_{ISCO}.

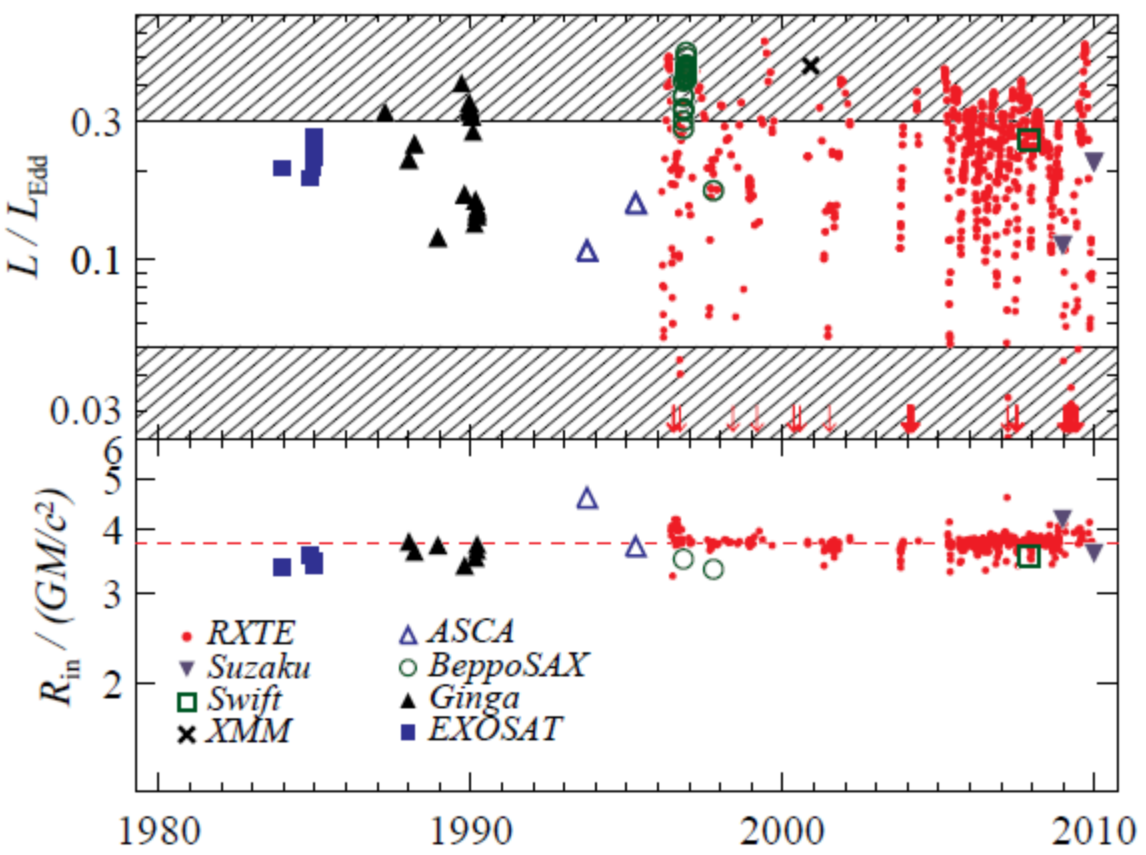

Fig. 5 (*top*) Accretion disk luminosity in Eddington-scaled units (for $M = 10\,M_\odot$) versus time for all the 766 spectra considered in a study of LMC X-3 by Steiner et al. (2010). (Downward arrows indicate data that are off scale.) Selected data in the unshaded region satisfy the thin-disk selection criterion $L/L_{Edd} < 0.3$ and avoid confusion with strongly-Comptonized hard-state data with $f_{SC} \gtrsim 25\%$ (Section 3.2; Remillard & McClintock 2006). (*bottom*) Fitted values of the inner-disk radius are shown for thin-disk data in the top panel that meet the selection criteria of the study (a total of 411 spectra). Despite large variations in luminosity, r_{in} remains constant to within a few percent over time. The median value for just the 391 selected *RXTE* spectra is shown as a red dashed line.

Table 7.3. Measured Values of BH Spins (a_*) Using the Continuum-fitting Method

Source	BH spin (a_*)	BH mass ($M_{BH}/M_\odot$)
Persistent X-ray binaries		
Cyg X-1	>0.9985*	21.2 ± 2.2
LMC X-1	$0.92^{+0.05}_{-0.07}$	10.9 ± 1.4
IC 10 X-1	$0.85^{+0.04}_{-0.07}$	15 (assumed)
M33 X-7	0.84 ± 0.05	15.65 ± 1.45
Transient X-ray binaries		
GRS 1915+105	>0.95	10.1 ± 0.6
MAXI J1803−298	0.991 ± 0.001	?
4U 1543−47	0.80 ± 0.10	9.4 ± 1.0
GRO J1655−40	0.70 ± 0.10	6.3 ± 0.5
Nova Mus 1991	$0.63^{+0.16}_{-0.19}$	11.0 ± 1.8
XTE J1550−564	$0.34^{+0.20}_{-0.28}$	9.1 ± 0.6
LMC X-3	<0.3	7.6 ± 1.6
H1743−322	0.2 ± 0.3	~ 8
MAXI J1820+070	$0.13^{+0.07}_{-0.10}$	8.5 ± 0.7
A0620−00	0.12 ± 0.19	6.6 ± 0.25

Source: After McClintock et al. (2014), Zhao et al. (2021), Reynolds (2021), Feng et al. (2021), Miller-Jones et al. (2021), and references therein.

*Assuming aligned spin ($\delta = 15°$ yields $a_* = 0.9696$; Miller-Jones et al., 2021).

Notice, no retrograde spins observed $\rightarrow$ $\vec{S} \parallel \vec{L}$ in progenitor star (and BH kick is small).

The BH spin can be estimated from:

1. X-ray continuum spectrum (e.g. McClintock, Narayan & Steiner 2013)
2. Relativistically broadened iron line (e.g. Reynolds 2013, 2021)
3. Quasi-periodic oscillations (?) (Dokuchaev 2013, Motta et al. 2014, 2022)

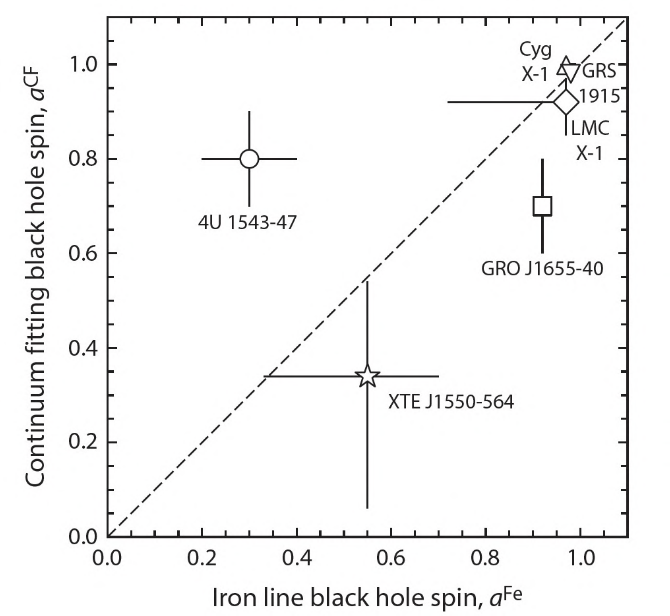

Salvesen & Miller (2021)

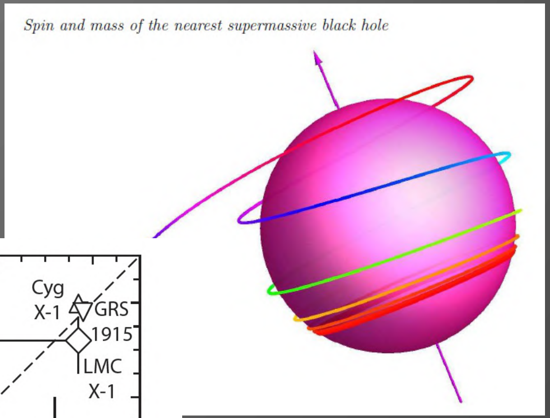

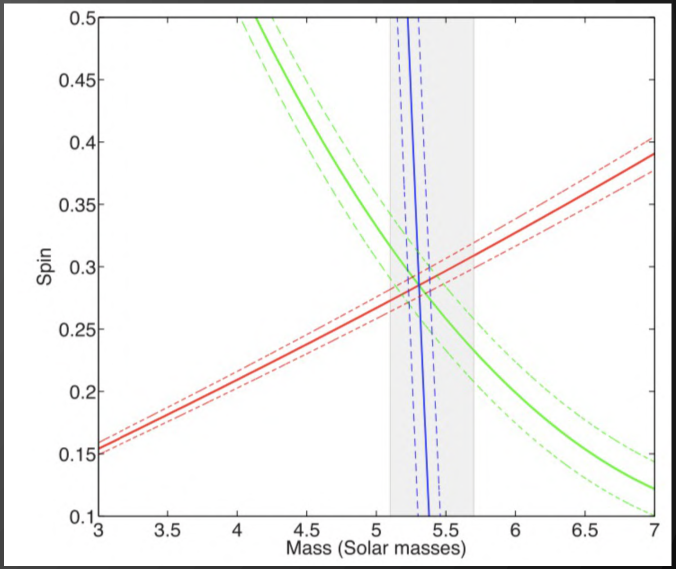

see next slide

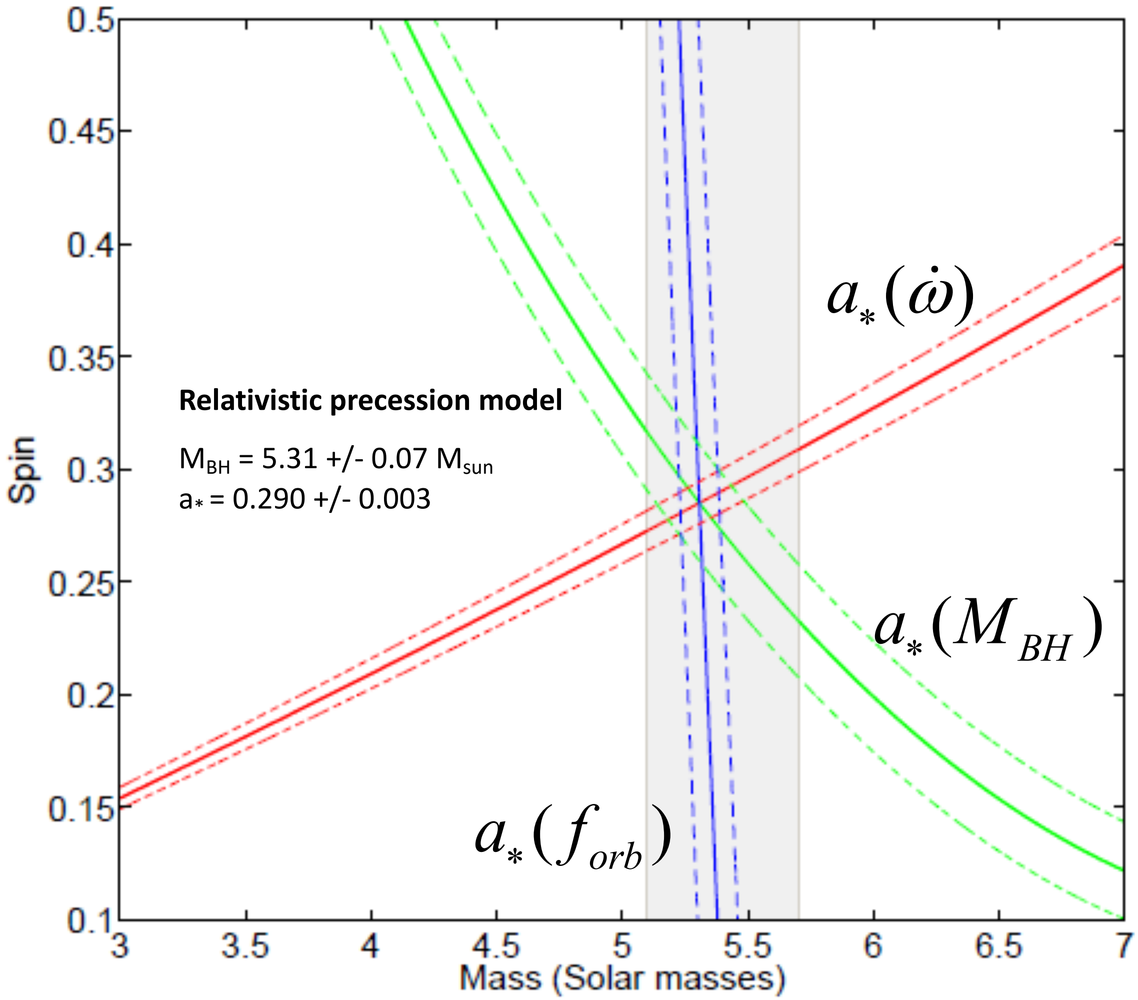

Motta, Belloni et al. (2014)

Figure 3. BH spin as a function of the mass as predicted by the three equations of the relativistic precession model for the BH binary GRO J1655-40. The derived BH parameters are mass = 5.31 ± 0.07 $M_\odot$ and spin a = 0.290 ± 0.003. The green, red and blue lines represent the spin as a function of the mass according to the functional form of the nodal precession, the periastron precession and the orbital frequency, respectively. The solid lines

The spins of the persistent BHs must be natal:

The accretion rate onto a BH is Eddington limited and the time interval of accretion is also limited by the age of the companion star.

Consider **Cyg X-1**:
To acheive $a_* > 0.95$ requires accretion of $> 7.3\, M_\odot$ if the BH was born non-spinning (Bardeen 1970; King & Kolb 1999).
For Eddington-limited accretion this requires: $\tau_{spin-up} \approx 31\, Myr$.
However, the age of the system is only $\tau_{nuc} \approx 4-7\, Myr$ (Wong et al. 2012).

Also for **M33 X-7** and **LMC X-1** is $\tau_{spin-up} \gg \tau_{nuc}$ (factor 5-6)
McClintock, Narayan & Steiner (2013).

Hence, these BH are *born rapidly spinning*.
(see also arguments in Mandel & Fragos 2020)

$$\frac{J}{J_{\rm BH}} \simeq \frac{1}{\chi}\,\frac{m}{M}\sqrt{\frac{R_{\rm ISCO}\,c^2}{GM}} \sim \frac{\sqrt{12}}{\chi}\,\frac{m}{M}.$$

(Tauris 2022)

Connecting BH spin and their jets:

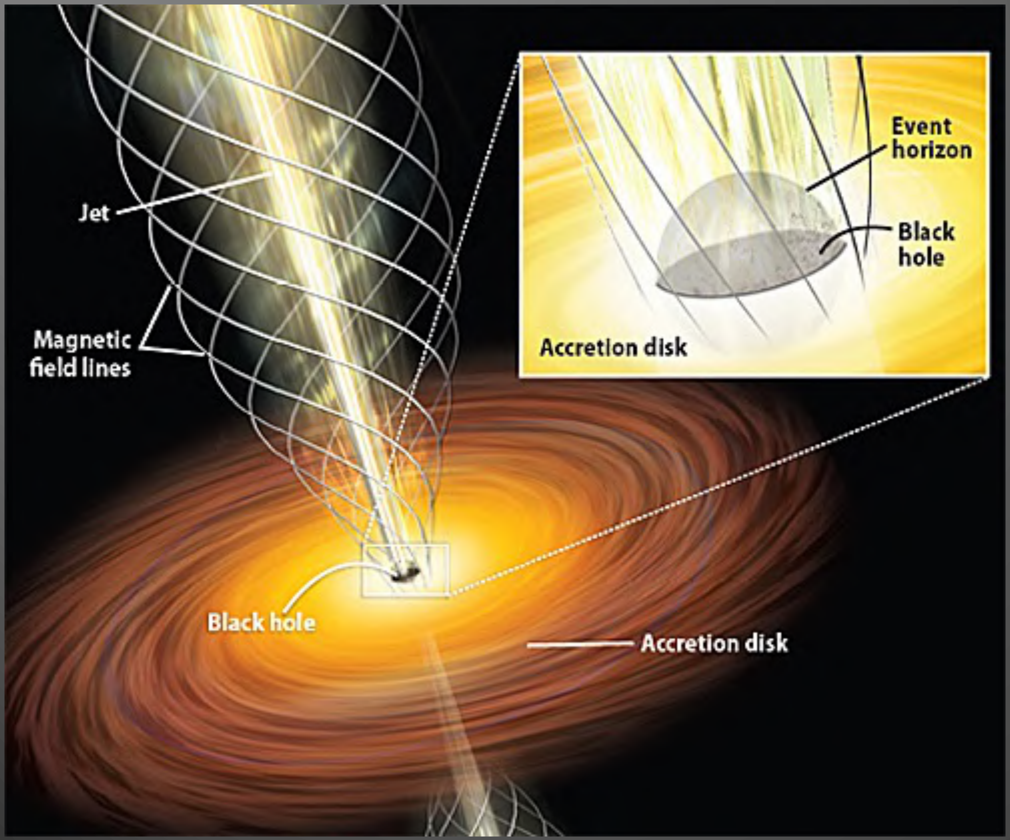

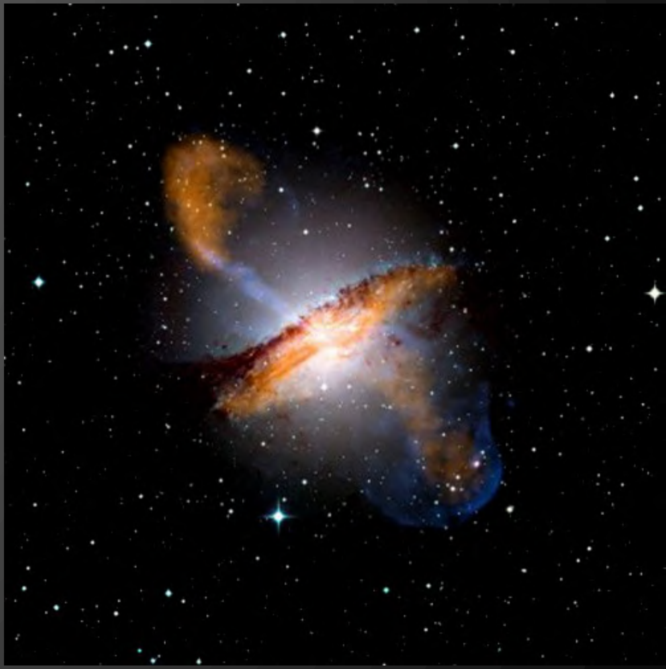

BHs may lose spin in jets

Poloidal B-field are twisted by frame-dragging, thereby producing outgoing Poynting flux along twin jets. Ruffini & Wilson (1975); Blandford & Znajek (1977)

Modern GRMHD simulations show that the power carried by the jet exceeds the total rest mass energy of accreted mass. Tchekhovskoy et al. (2011)

$$\eta_{jet} \equiv \left\langle L_{jet} \right\rangle / \dot{M}c^2$$

McClintock, Narayan & Steiner (2013)

$$\eta_{jet} \propto \Omega_H^2$$

$$\Omega_H = \frac{c^3}{2GM}\left(\frac{a_*}{1+\sqrt{1-a_*^2}}\right)$$

Angular velocity at the BH horizon

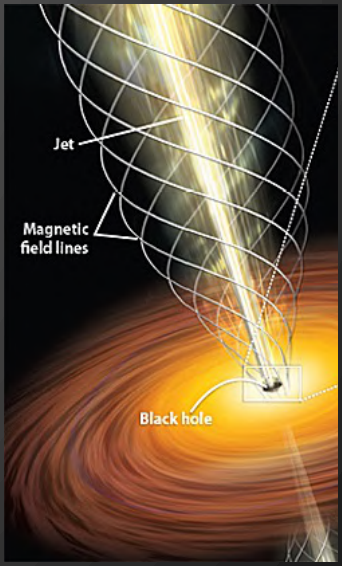

$\eta_{jet} \propto a_*^2$

$\eta_{jet} \propto \Omega_H^2$

20

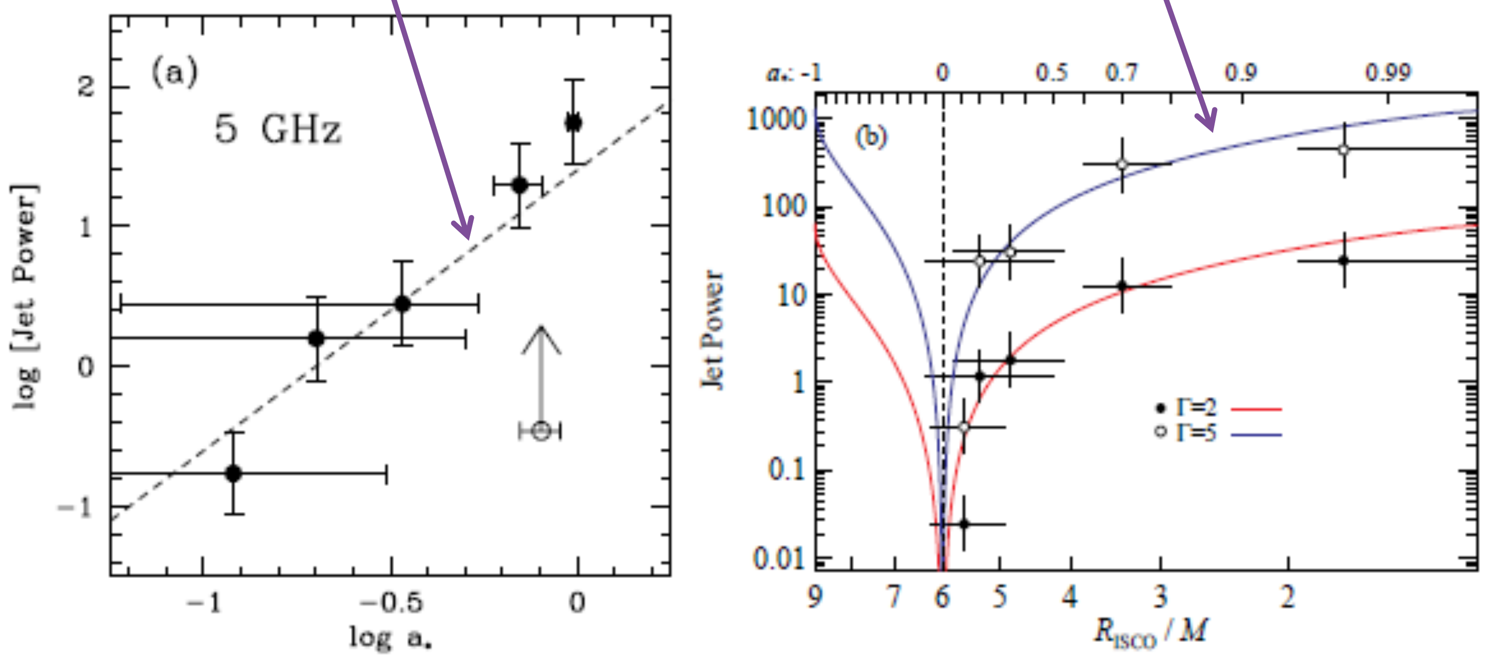

Fig. 6 (a) Plot of the quantity Jet Power, which measures the 5 GHz radio luminosity at light curve maximum, versus black hole spin, measured via the continuum-fitting method for five transients (Narayan & McClintock 2012; Steiner et al. 2013). The dashed line has slope equal to 2. (b) Plot of Jet Power versus $R_{\rm ISCO}/(GM/c^2)$. Here the radio luminosity has been corrected for beaming assuming a bulk Lorentz factor $\Gamma = 2$ (filled circles) or $\Gamma = 5$ (open circles). The solid lines correspond to Jet Power $\propto \Omega_{\rm H}^2$, where $\Omega_{\rm H}$ is the angular frequency of the horizon (Steiner et al. 2013).

However, see also critique by Fender et al. (2010) and Russell et al. (2013)

BHs may lose spin in jets

Poloidal B-field are twisted by frame-dragging, thereby producing outgoing Poynting flux along twin jets. Ruffini & Wilson (1975); Blandford & Znajek (1977)

Modern GRMHD simulations show that the power carried by the jet exceeded the total rest mass energy of accreted mass. Tchekhovskoy et al. (2011)

$$\eta_{jet} \equiv \langle L_{jet} \rangle / \dot{M}c^2$$

McClintock, Narayan & Steiner (2013)

$$\eta_{jet} \propto \Omega_H^2$$

$$\Omega_H = \frac{c^3}{2GM}\left(\frac{a_*}{1+\sqrt{1-a_*^2}}\right)$$

Angular velocity at the BH horizon

For Cyg X-1: $P_H \approx 1.3\ ms$

Accretion disk winds may eject a significant of the transfered material

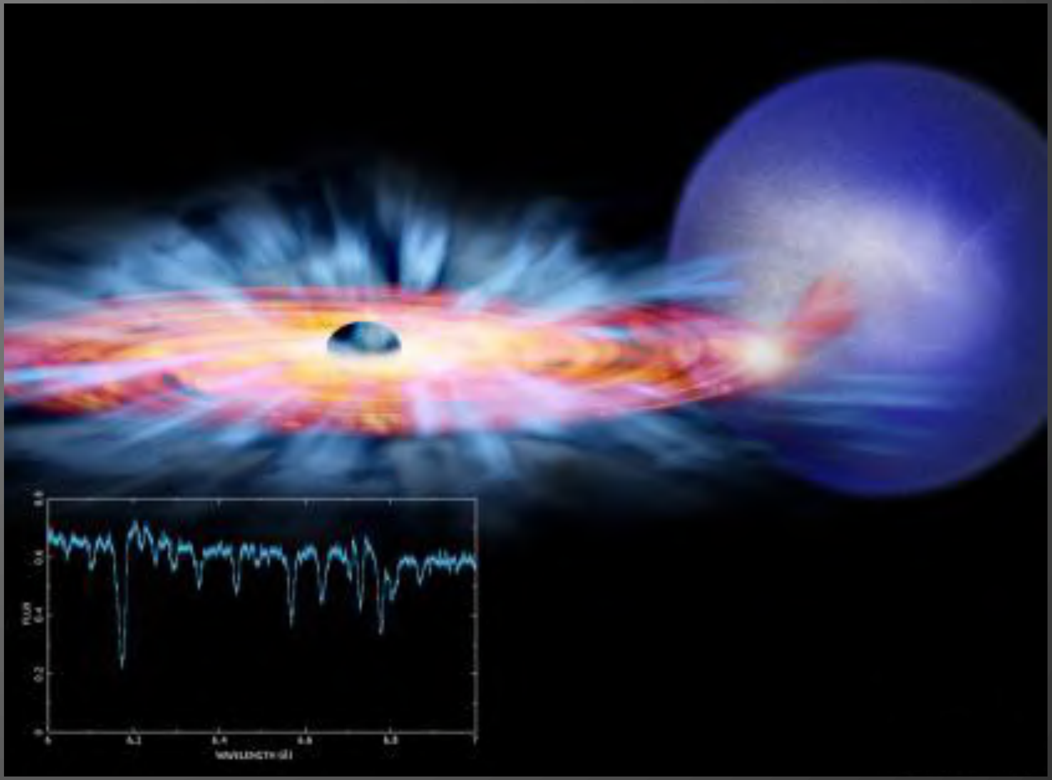

Determination of BH masses via mass function

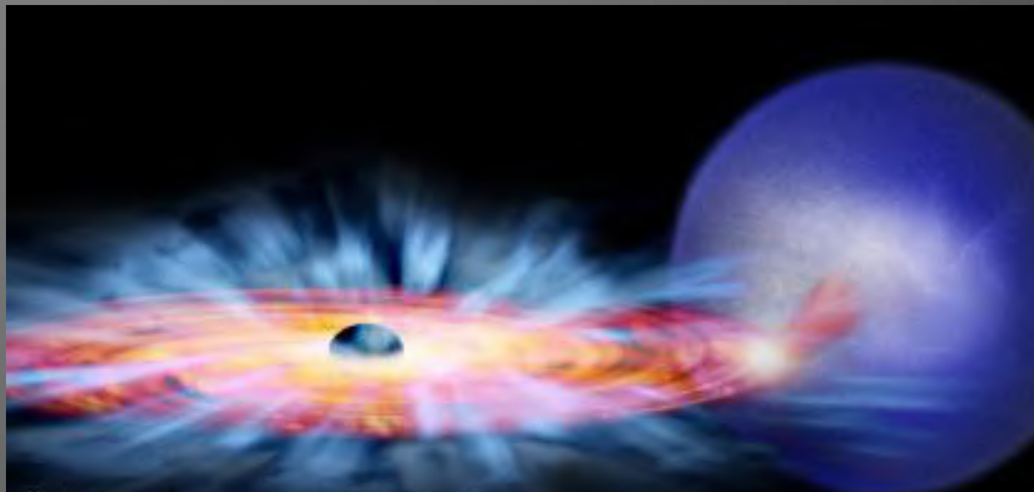

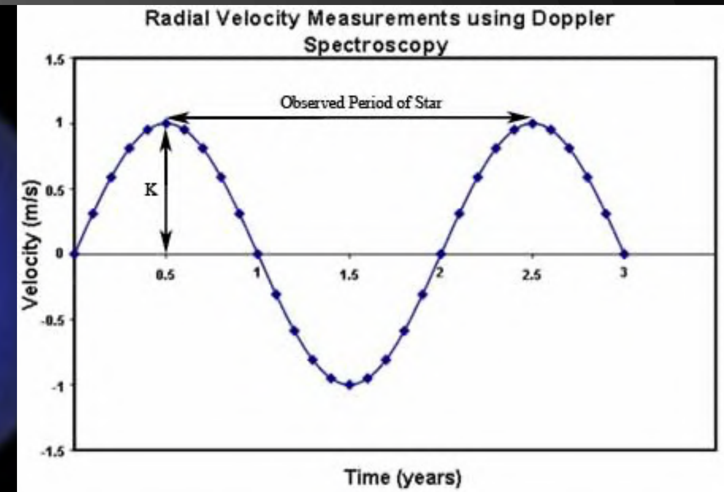

$$f(M) \equiv \frac{4\pi^2 (a_X \sin i)^3}{G P_{orb}^2} = \frac{M_2^3 \sin^3 i}{(M_X + M_2)^2}$$

In practice, one measures the radial velocity amplitude: $K_X = \dfrac{\Omega a_X \sin i}{\sqrt{1-e^2}}$

Hence, the estimated BH mass strongly depends on the (often) unknown orbital inclination angle, i.

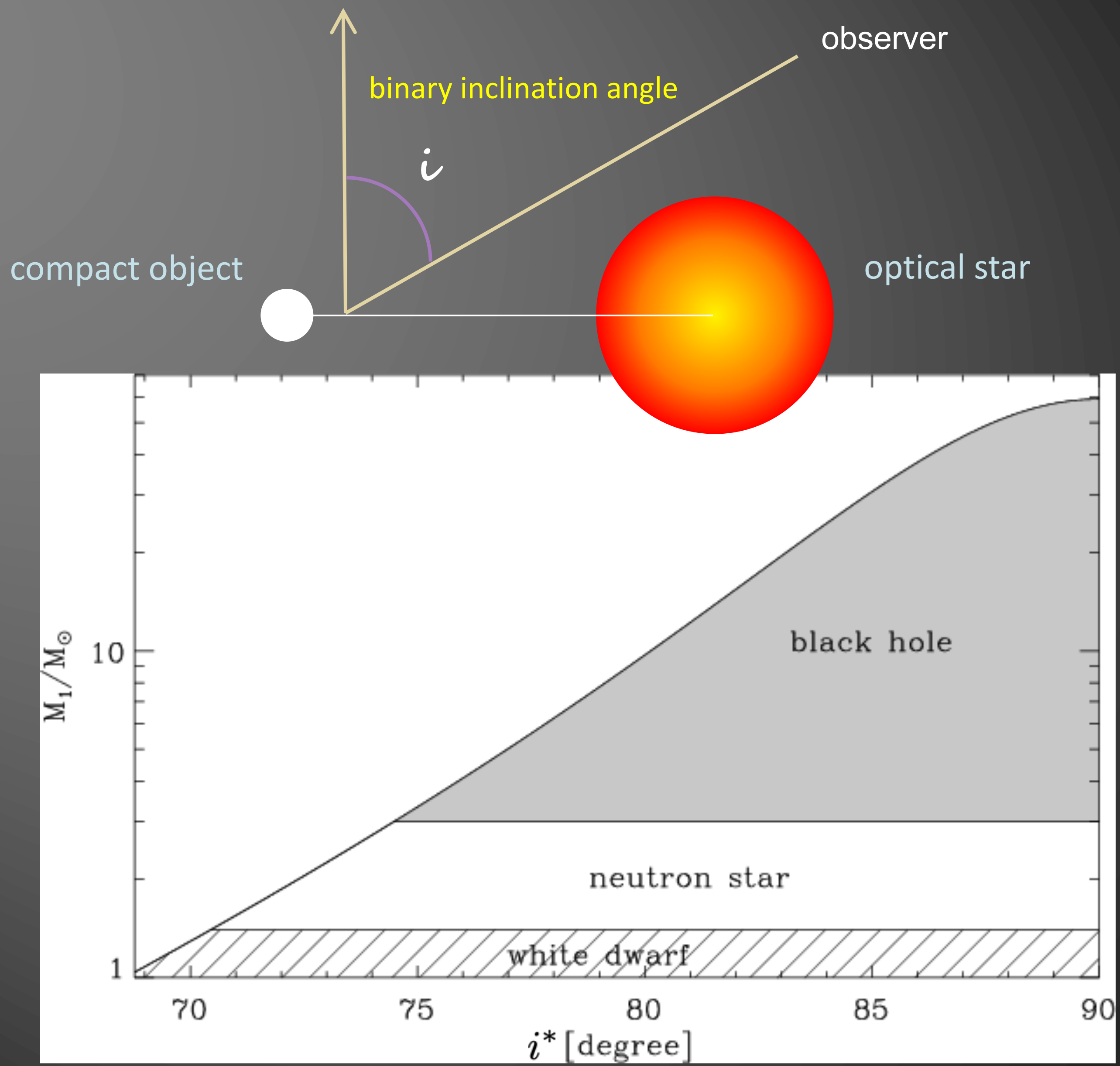

Note:
here is plotted

$$i^* = \frac{\pi}{2} - i$$

Sometimes it is difficult to determine if the accreting object is a NS or a BH.

Ballistic jets and microquasars

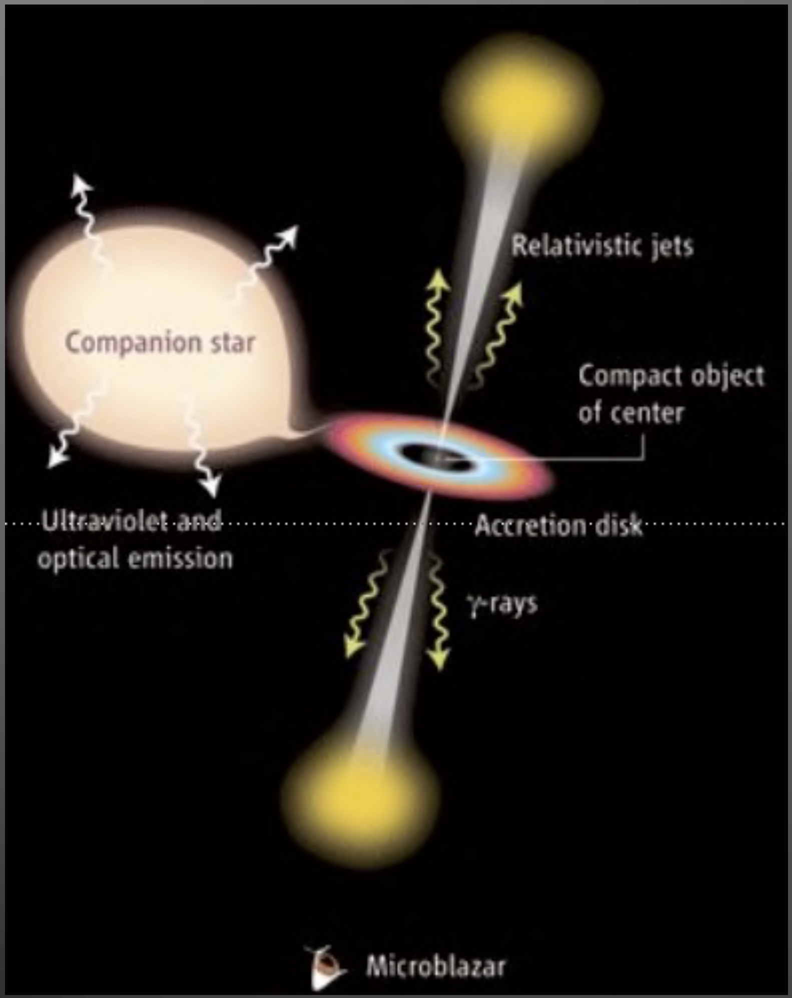

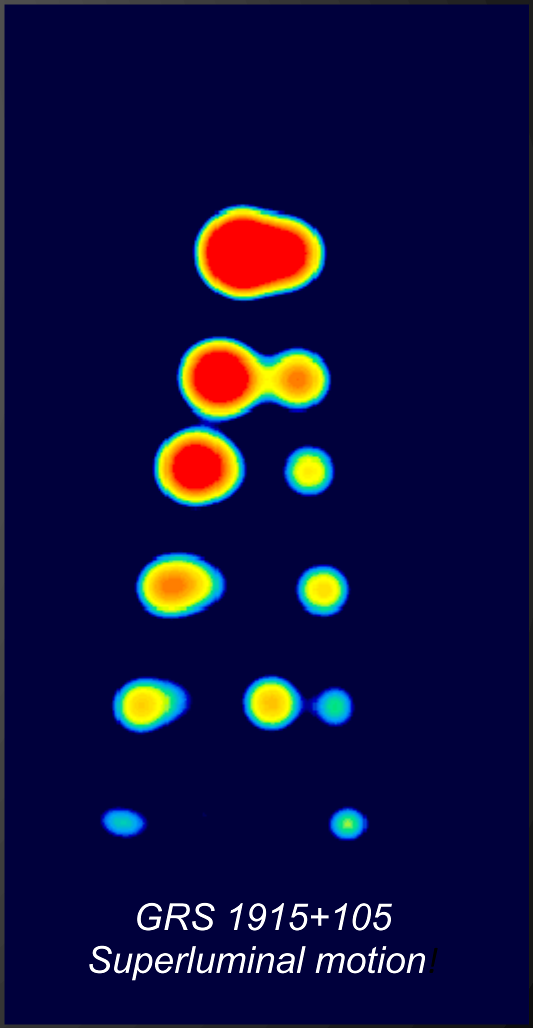

GRS 1915+105
Superluminal motion

BH: radio/X-ray luminosity correlation

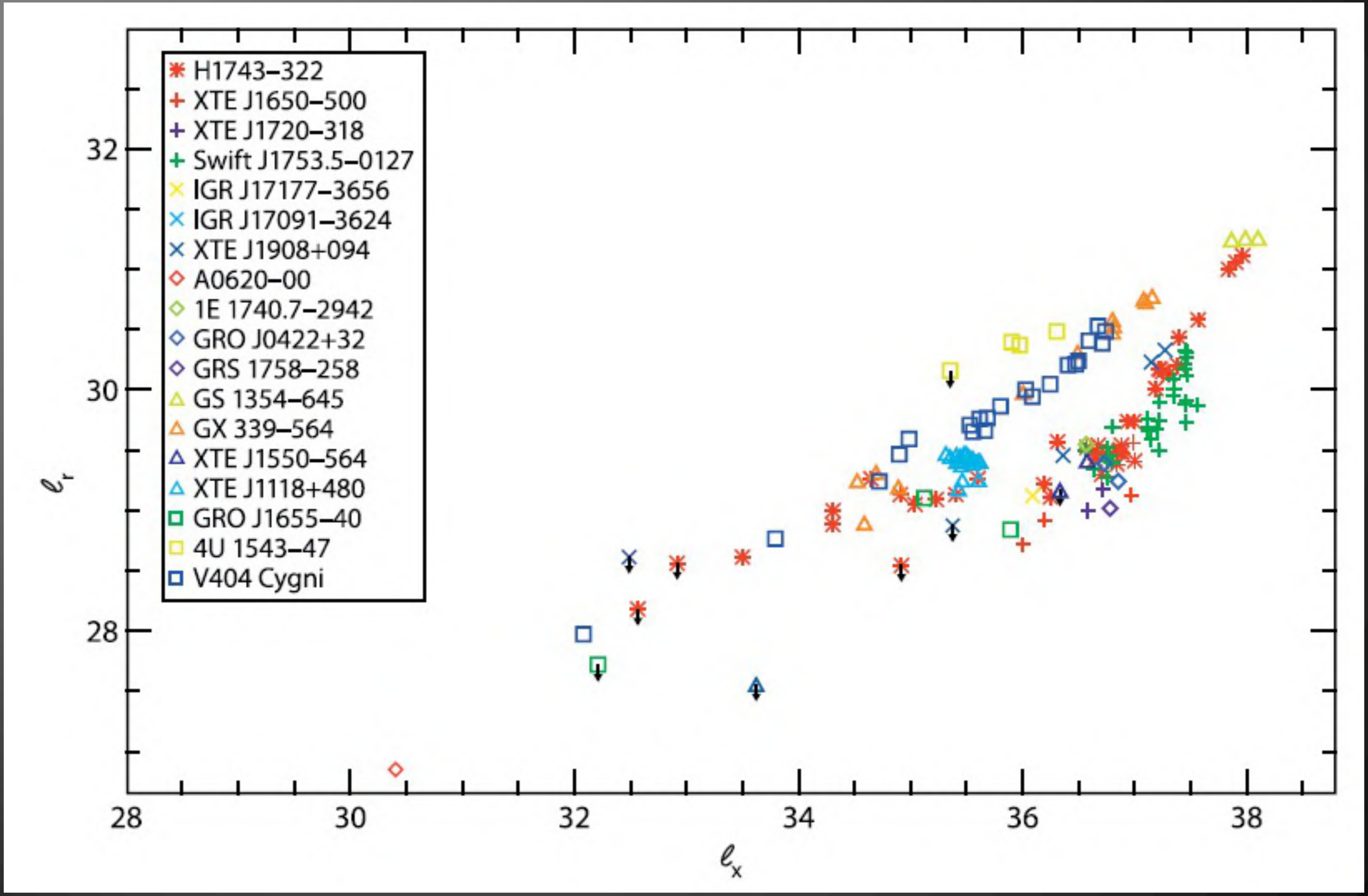

Gallo, Fender & Pooley (2003), Coriat et al. (2011), Meyer-Hoffmeister & Meyer (2014)

Summary

Summary

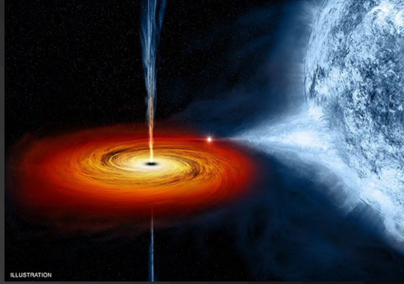

- Stellar mass BHs have spins: $0.1 < a_* < 0.99 \quad \wedge \quad a_* \equiv \dfrac{cJ}{GM^2}$
- BH spins can be determined via the continuum-fitting model

Next Week

- BH spins can also be measured in merging BH binaries (LIGO)
- The two classes of BHs (transient vs persistent) have different spins
- The fast spins of the persistent BHs are natal
- The BH spins seem to be correlated with the jet power

Literature

- Shapiro & Teukolsky (1983), Chapter 12 (14)
- McClintock, Narayan & Steiner (2013)
- Fabian & Lasenby (2015)
- R. Shafee (2008), Measuring Black Hole Spin, PhD Thesis, Chapter 1+2
- LIGO consortium (2016), "*Observations of Gravitational Waves…*" http://arxiv.org/abs/1602.03837

Programme

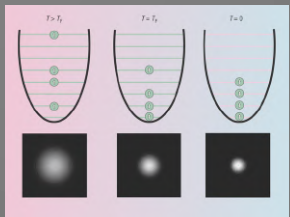


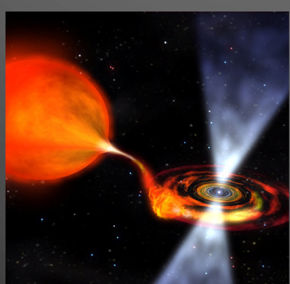


- **Introduction**
- **Degenerate Fermi Gases**
  Non-relativistic and extreme relativistic electron / (n,p,e^-) gases
- **White Dwarfs**
  Structure, cooling models, observations
- **Neutron Stars**
  Structure and equation-of-state
- **Radio Pulsars**
  Characteristics, spin evolution, magnetars, observations
- **Binary Evolution and Interactions**
  X-ray binaries, accretion, formation of millisecond pulsars, recycling
- **Black Holes**
  Observations, characteristics and spins
- **Gravitational Waves**
  Sources and detection, kilonovae
- **Exam**

Physics of Compact Objects
week 9

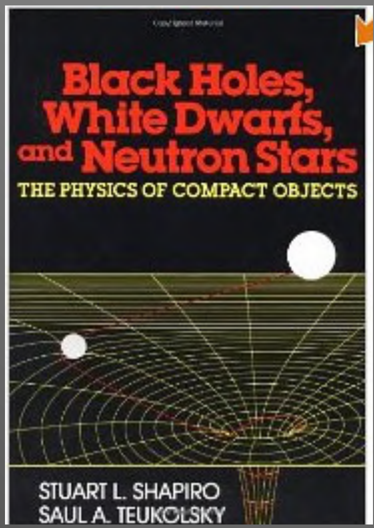

Shapiro & Teukolsky (1983), Wiley-Interscience

Curriculum
- Lecture notes
  + Tauris & van den Heuvel (2023): Chapter 7.6
  + McClintock et al. (2013)
  (Reynolds 2021; Fabian & Lasenby 2015)
  (Shapiro & Teikolsky Chapter 12 (14))

Exercises: # 17, 18 + four phases of accretion

- Monday Nov. 6, 10:15-12:00

Next lecture: Gravitational waves
- Mon. Nov.12, 08:15-10:00, Aud. 2.115
- Tauris & van den Heuvel (2023), Chapter 15
  (Riles 2013; Colpi & Sesana 2017)